

## **Distribution Agreement**

In presenting this thesis or dissertation as a partial fulfillment of the requirements for an advanced degree from Emory University, I hereby grant to Emory University and its agents the non-exclusive license to archive, make accessible, and display my thesis or dissertation in whole or in part in all forms of media, now or hereafter known, including display on the world wide web. I understand that I may select some access restrictions as part of the online submission of this thesis or dissertation. I retain all ownership rights to the copyright of the thesis or dissertation. I also retain the right to use in future works (such as articles or books) all or part of this thesis or dissertation.

Signature:

---

Xuan Yang

---

Date

Validation of MKK3/MYC PPI as a Potential Therapeutic Target

By

Xuan Yang

Master of Science

Graduate Division of Biological and Biomedical Science

Cancer Biology and Translational Oncology

---

Haian Fu, Ph.D.

Advisor

---

Andrey Ivanov, Ph.D.

Committee Member

---

Xingming Deng, MD, Ph.D.

Committee Member

---

Lily Yang, MD, Ph.D.

Committee Member

Accepted:

---

Lisa A. Tedesco, Ph.D.

Dean of the James T. Laney School of Graduate Studies

---

Date

Validation of MKK3/MYC PPI as a Potential Therapeutic Target

By

Xuan Yang

B.S., Emory University, 2018

Advisor: Haian Fu, Ph.D.

An abstract of  
A thesis submitted to the Faculty of the  
James T. Laney School of Graduate Studies of Emory University  
in partial fulfillment of the requirements for the degree of  
Master of Science  
in the Graduate Division of Biological and Biomedical Science  
Cancer Biology and Translational Oncology  
2019

## Abstract

### Validation of MKK3/MYC PPI as a Potential Therapeutic Target

By Xuan Yang

Oncogenic master transcription factor MYC is amplified in nearly all cancers. However, MYC lacks known enzymatic activity and its targeting by small molecules is highly challenging. Meanwhile, MYC transcription activity is controlled by other proteins through the regulation of its protein level and expression. Previously, mitogen-activated protein kinase kinase 3 (MKK3) has been identified as a novel binding partner of the major tumor driver MYC. The protein-protein interaction (PPI) between MKK3 and MYC leads to upregulation of MYC transcriptional activity in cancer cells. We discovered that ASK1 (MAP3K5) a major activator of MKK3 can serve as a potential regulatory switch between MKK3 pro-inflammatory and pro-apoptotic p38 MAPK activation and oncogenic activation of MYC. GSK3 $\beta$ , a negative regulator that promotes MYC degradation, has also been identified as a novel binding partner of MKK3. We found that inhibition of GSK3 $\beta$ -dependent MYC degradation is a potential mechanism MKK3 uses to enhance MYC stability. These data provide new mechanistic insights into MKK3-dependent MYC activation. To interrogate MKK3/MYC binding interface I developed inhibitory peptides derived from MYC HLH domain. Antitumor effect of the peptides suggests that MKK3/MYC PPI is druggable and its inhibition has potential therapeutic effect. Through the high-throughput screening of compounds with known bioactivity we have discovered first-in-class inhibitors for MKK3/MYC PPI, including the quinoline derivative SGI-1027. Previous studies defined SGI-1027 as a probe for DNA methyltransferase activity, however other biological targets for this molecule remained unexplored. we found that SGI-1027 inhibits MKK3/MYC PPI in multiple assays at low micromolar range, and demonstrates selectivity against other well-defined MYC and MKK3 PPIs, such as MYC/MAX and MKK3/p38 PPIs. Disruption of MKK3/MYC PPI correlates with the suppression of MYC transcriptional activity and reduced proliferation in multiple cancer cell lines. Together, our findings define MKK3/MYC PPI interface as a new promising target to regulate MYC activation. These data build a strong basis for further investigation of MKK3/MYC PPI dependency for therapeutic discovery in cancer.

Validation of MKK3/MYC PPI as a Potential Therapeutic Target

By

Xuan Yang

B.S., Emory University, 2018

Advisor: Haian Fu, Ph.D.

A thesis submitted to the Faculty of the  
James T. Laney School of Graduate Studies of Emory University  
in partial fulfillment of the requirements for the degree of  
Master of Science  
in the Graduate Division of Biological and Biomedical Science  
Cancer Biology and Translational Oncology  
2019

## Acknowledgements

The Fu Lab and Emory Chemical Biology Discovery Center:

Haian Fu, Ph.D.

Yuhong Du, Ph.D.

Andrey A. Ivanov, Ph.D.

Qiankun Niu, Ph.D.

Xiulei Mo, Ph.D.

Kun Qian, Ph.D.

Valentina González-Pecchi

Min Qui

Cong Tang

Shiping Zhang

Sean P. Doyle

Danielle Cicka

Sha Fu

Changfa Shu

Li Zhang

Ling Gu

Brian Revennaugh

Former Lab Members:

Qi Qi, Ph.D.

Jinglin Xiong, MD, Ph.D.

Jun Shi, MD, Ph.D.

Lauren Rusnak Ph.D.

Thesis Committee:

Xingming Deng, MD, Ph.D.

Lily Yang, MD, Ph.D.

Laney Graduate School, Graduate Division of Biological and Biomedical Sciences

Winship Cancer Institute

Emory University Research Committee

NIH Cancer Target Discovery and Development Network

## Table of Contents

<b>Introduction</b>	<b>1</b>
PPIs as Promising Targets for Therapeutic Discoveries	2
MYC as a Tough Target Associated with Various Diseases	3
Targeting MYC for Therapeutic Development Remains Challenging	4
OncoPPI-informed discovery of MKK3 as a Novel Binding Partner of MYC	5
MKK3/MYC PPI Validations	6
Interrogation of MKK3/MYC PPI Interface	7
Functional Studies Indicate MKK3/MYC PPI as a Potential Therapeutic Target	8
Scope of the Thesis	9
<b>Materials and Methods</b>	<b>12</b>
Reagents	13
Cell Line and Culture Conditions	13
DNA Constructs	14
GST-pull down Assay	14
Western Blot	14
TR-FRET Measurements	15
Development of MKK3/MYC TR-FRET Assay in a 384-Well HTS Format	15
Miniaturization of the Assay into a 1,536-Well uHTS Format	16
Pilot Screening for Potential MKK3/MYC Inhibitors through uHTS in a 1536-Well Format	17
Dose-Response TR-FRET Validation for Compound Hits	17

Data analysis	18
MYC reporter assay	19
Computational modeling	19
<b>Results</b>	<b>20</b>
Shorter truncations were designed and generated from MYC bHLH domain	21
MKK3/MYC PPI can be disrupted by inhibitory peptides	22
Overexpression of MKK3/MYC inhibitory peptide correlates with anti-tumor effects	22
Further narrow-down of MKK3-binding site on MYC	25
Development of the ultra-high-throughput screening assay for MKK3/MYC PPI inhibitors	26
The uHTS screening for MKK3/MYC PPI inhibitors	28
Validation of SGI-1027 as the disruptor of MKK3/MYC PPI	30
SGI-1027 shows significant MKK3/MYC PPI selectivity	33
Computational modeling reveals SGI-1027-binding site on MKK3	36
SGI-1027 suppresses MYC transcriptional activity and proliferation of cancer cell lines	37
MKK3 knock-down results in decreased MYC transcriptional activity	39
Suppressive effect of SGI-1027 on MYC activity and cell proliferation correlates with inhibition of MKK3/MYC PPI	39
Identification of potential regulators for MKK3/MYC PPI	42
ASK1 is a potential modulator of MKK3/MYC PPI	42
MKK3 interferes with MYC/GSK3 $\beta$ interaction	45

Discussion	47
Future directions	52
References	53

### Table of Figures

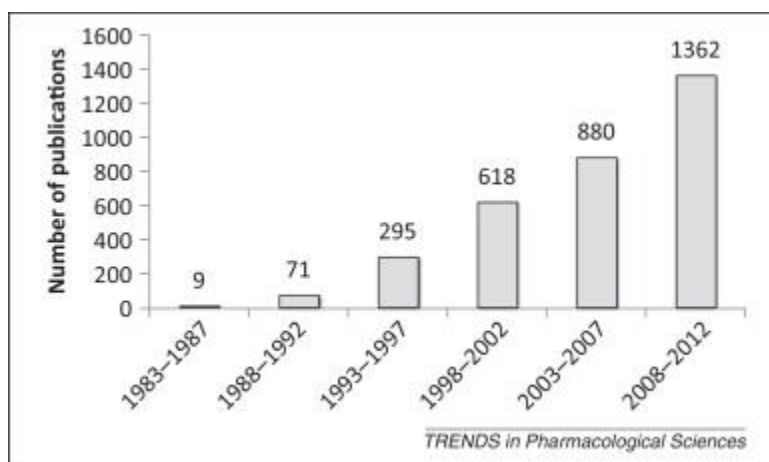
Figure 1. Protein-protein interactions emerging as promising targets.	2
Figure 2. Master transcription factor MYC is tightly related to tumorigenesis.	3
Figure 3. Co-crystallization reveals binding characteristics for MYC/MAX PPI.	4
Figure 4. MKK3 (MAP2K3) identified as a major hub in the OncoPPI network.	5
Figure 5. MKK3/MYC PPI was validated in multiple orthogonal assays.	6
Figure 6. Identification of binding-domains on MKK3 and MYC responsible for their interaction	7
Figure 7. MKK3 inhibits MYC degradation and upregulates its activity.	9
Figure 8. Identification of MKK3-binding site on MYC HLH-domain.	21
Figure 9. MYC 370-413 selectively inhibits the interaction between MKK3 and MYC.	23
Figure 10. Overexpression of peptide antagonist correlates with anti-tumor effect in cancer cells.	24
Figure 11. MKK3-binding domain on MYC narrowed down to MYC 380-406.	25

Figure 12. Evaluation of the MKK3/MYC PPI TR-FRET assay.	27
Figure 13. Pilot uHTS screening for MKK3/MYC PPI inhibitors.	29
Figure 14. Dose-response validation of primary hits detected in uHTS assay.	31
Figure 15. Orthogonal validations of SGI-1027 as MKK3/MYC PPI inhibitor.	32
Figure 16. SGI-1027 does not disrupt the PPIs between major MKK3 and MYC binding partners.	34
Figure 17. SGI-1027 showed selectivity against other MKK3 PPIs.	35
Figure 18. Molecular computational modeling reveals SGI-1027-binding site on MKK3.	36
Figure 19. SGI-1027 suppresses MYC transcriptional activity and proliferation of cancer cell lines.	38
Figure 20. MKK3 knock-down results in decreased MYC transcriptional activity.	40
Figure 21. Sensitivity of HCT116 cells to SGI-1027 is MKK3 dependent.	41
Figure 22. ASK1 and GSK3 $\beta$ can inhibit MKK3/MYC PPI.	43
Figure 23. ASK1 is verified as a potential modulator of MKK3/MYC PPI.	44
Figure 24. MKK3 promotes MYC stability through inhibiting GSK3 $\beta$ -dependent MYC degradation.	46

# **INTRODUCTION**

## PPIs as Promising Targets for Therapeutic Discoveries

As people's knowledge about cancer biology develops, a better understanding of protein-protein interactions (PPIs) as promising targets with relatively less investigation leads to the rapid growth of interest in the field of cancer-related PPIs. PPIs play a pivotal role in all cellular programs, including cell growth and survival<sup>1</sup>. However, elucidation of specific functions mediated by a particular PPI is challenging, especially for non-enzyme proteins, such as transcription factors that are often considered as “undruggable”<sup>2-5</sup>. Development of PPI-specific small molecule chemical probes can tremendously facilitate our understanding of biological pathways leading to new therapeutic strategies<sup>1,6,7</sup>.



Ivanov *et al.*, 2013

**Figure 1. Protein-protein interactions emerging as promising targets.** Rising number of publications in the field of cancer-related protein-protein interactions<sup>1</sup>.

## MYC as a Tough Target Associated with Various Diseases

Overexpression of the transcription factor MYC has a close relationship with the elevated level of cell cycle progression, and cell cycle related genes are tightly regulated by MYC<sup>8</sup> (Fig. 2A). As one of the most frequently altered tumor drivers, MYC amplification and overexpression correlates with poor patient survival in different tumor types<sup>9-15</sup> (Fig. 2B). It was estimated that MYC causes more than 1,000,000 people death every year<sup>16</sup>. Furthermore, MYC plays a key role in upregulation of vascular smooth muscle cell proliferation that leads to thickening of the inner layer of blood vessels and development of coronary artery disease and heart failure<sup>17-19</sup>. Currently, MYC is a validated target for a range of human diseases, such as cancer, neurodegenerative Alzheimer's, Parkinson's, and Huntington's diseases, and cardiovascular disorders<sup>20-22</sup>.

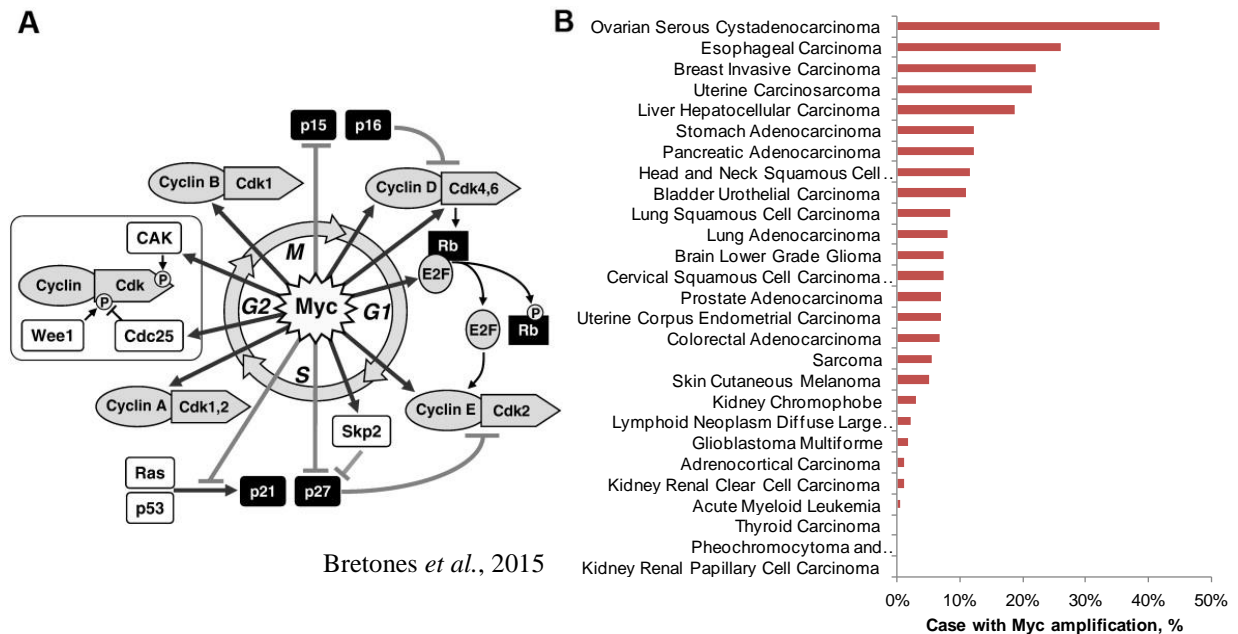
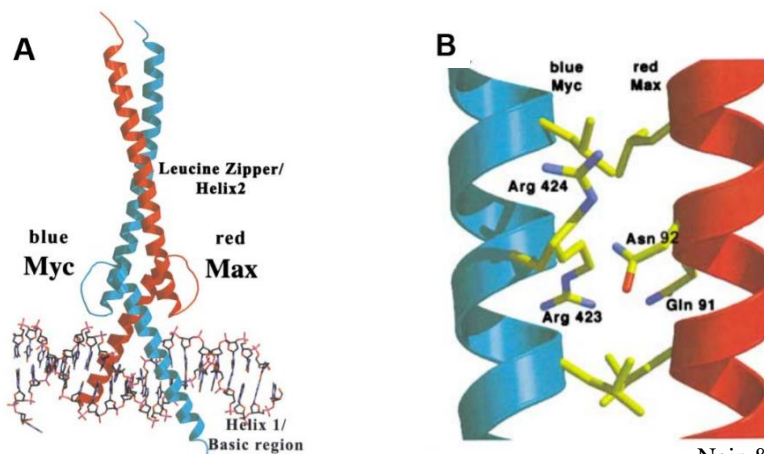


**Figure 2. Master transcription factor MYC is tightly related to tumorigenesis.** A) Myc stimulates the cell cycle progression. Schematic representation of the cell cycle phases, the main cell cycle regulators and how Myc influence the cell cycle through the induction or repression of target genes encoding many of those regulators<sup>8</sup>. B) TCGA data suggest a strong correlation between Myc amplification and cancer incidence.

## Targeting MYC for Therapeutic Development Remains Challenging

MYC lacks any known enzymatic function, and its transcription activity is controlled by other proteins through the regulation of its protein level and expression<sup>23,24</sup>. For example, regulation of MYC stability by ERK and GSK3 $\beta$  kinases through phosphorylation of MYC Thr58 and Ser62 residues, and its dephosphorylation by phosphatase 2A (PP2A) play prominent roles in MYC-driven tumorigenesis<sup>25</sup>. The C-terminal part of MYC contains a basic HLH-LZ domain, which is largely unstructured until it dimerizes with other partners, such as MAX to bind DNA promoters at the enhancer (E)-boxes with a canonical CAC(G/A)TG sequence<sup>26</sup> (Fig. 3A-B). Thus, perturbation of MYC protein-protein interactions has emerged as the promising strategy to target MYC for cancer therapeutic discovery<sup>27,28</sup>. However, targeting MYC with small molecules remains highly challenging<sup>4,29</sup>. MYC is frequently amplified, but its low incidence of mutation as well as its universal role to cell proliferation lead to criticisms against development of MYC inhibitors<sup>27</sup>. Currently no FDA-approved MYC PPI inhibitors are available and new strategies to regulate MYC PPIs are highly needed to facilitate therapeutic development for MYC-driven cancer.



Nair & Burley, 2003

**Figure 3. Co-crystallization reveals binding characteristics for MYC/MAX PPI.** A) The overall topology of the Myc-Max/DNA cocrystal structures. Color coding: Myc-cyan, Max-red. Co-crystallization oligonucleotide is shown as an atomic stick figure. The helix, basic region, and zipper regions have been designated on the Myc-Max/DNA structure<sup>26</sup>. B) Ribbon diagram of the Myc-Max heterodimer (Myc-blue; Max-red). Hydrogen bond pairs created by the disposition of Gln-Asn-Arg-Arg residues in the tetrad region yield a tighter dimer interface<sup>26</sup>.

## OncoPPI-informed discovery of MKK3 as a Novel Binding Partner of MYC

Recently, our group identified Mitogen Activated Protein Kinase Kinase 3 (MKK3) as a major hub in the OncoPPI network<sup>30,31</sup>. High-throughput screening for protein-protein interactions revealed more than twenty proteins that binds to MKK3 (Fig. 4A). Many signaling pathways are related to the newly discovered MKK3-binding partners, such as STK11-induced autophagy, HIF1-mediated Warburg effect and angiogenesis, CDK4-induced cell cycle progression, and so on (Fig. 4B). Among those, MYC caught our attention since there were no report about the crosstalk between MAP kinase signaling pathway and the master transcription factor MYC. If true, this PPI might provide new mechanisms for MYC regulation, besides the well investigated MYC/MAX interaction.

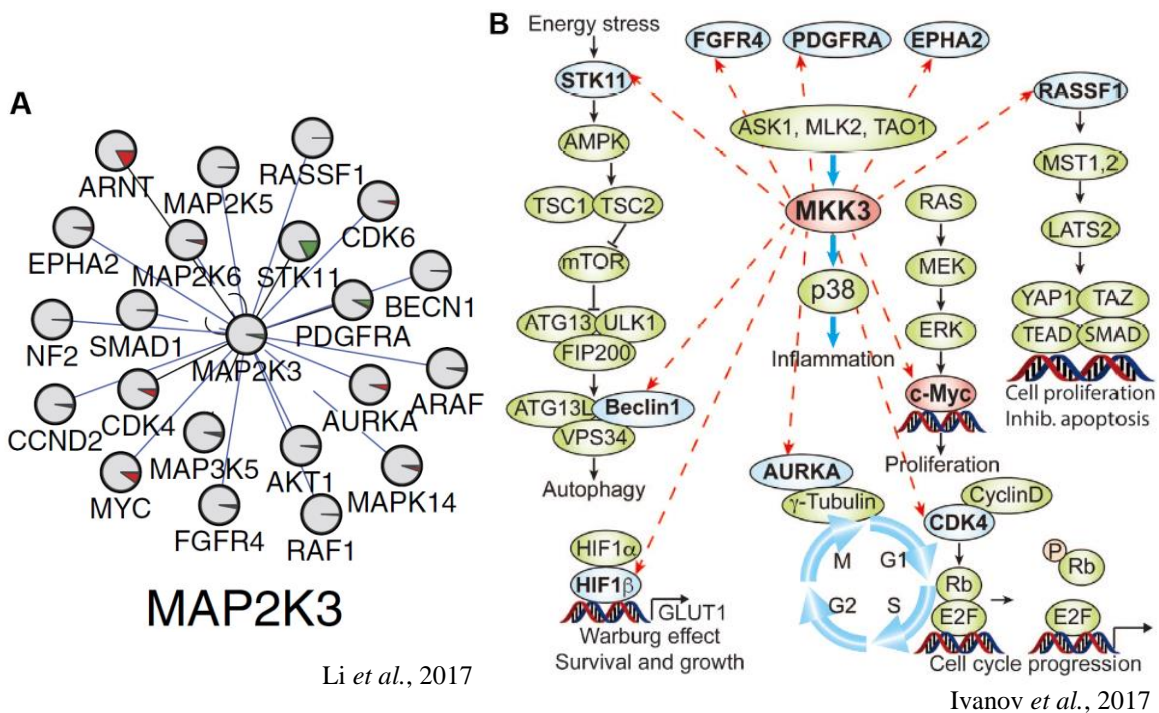


**Figure 4. MKK3 (MAP2K3) identified as a major hub in the OncoPPI network.** A) Hub and spoke diagram for MAP2K3 in the OncoPPI network. The red, blue and green sectors inside the nodes represent the percent of LUAD cases (based on LUAD TCGA provisional dataset) with gene amplifications, deletions or mutations, respectively<sup>30</sup>. B) Diagram showing new MKK3 binding partners and associated pathways<sup>31</sup>.

## MKK3/MYC PPI Validations

Besides the TR-FRET assay that was originally used to discover the interaction between MKK3 and MYC, this PPI was further validated in multiple orthogonal assays, including GST pull-down and endogenous co-immunoprecipitation (Fig. 5A-C). Venus PCA assay also demonstrated that this particular interaction happens in live cells (Fig. 5D).

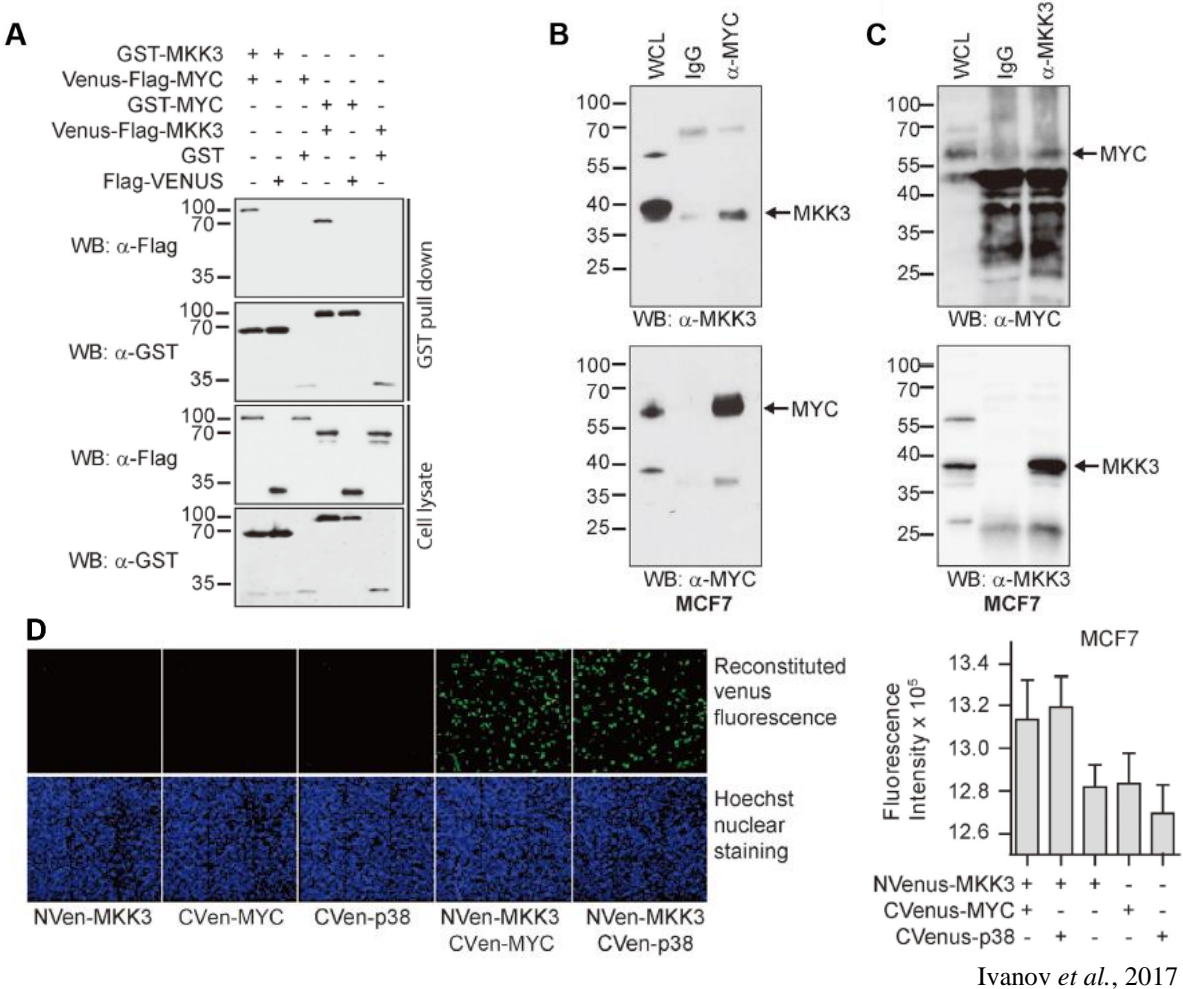
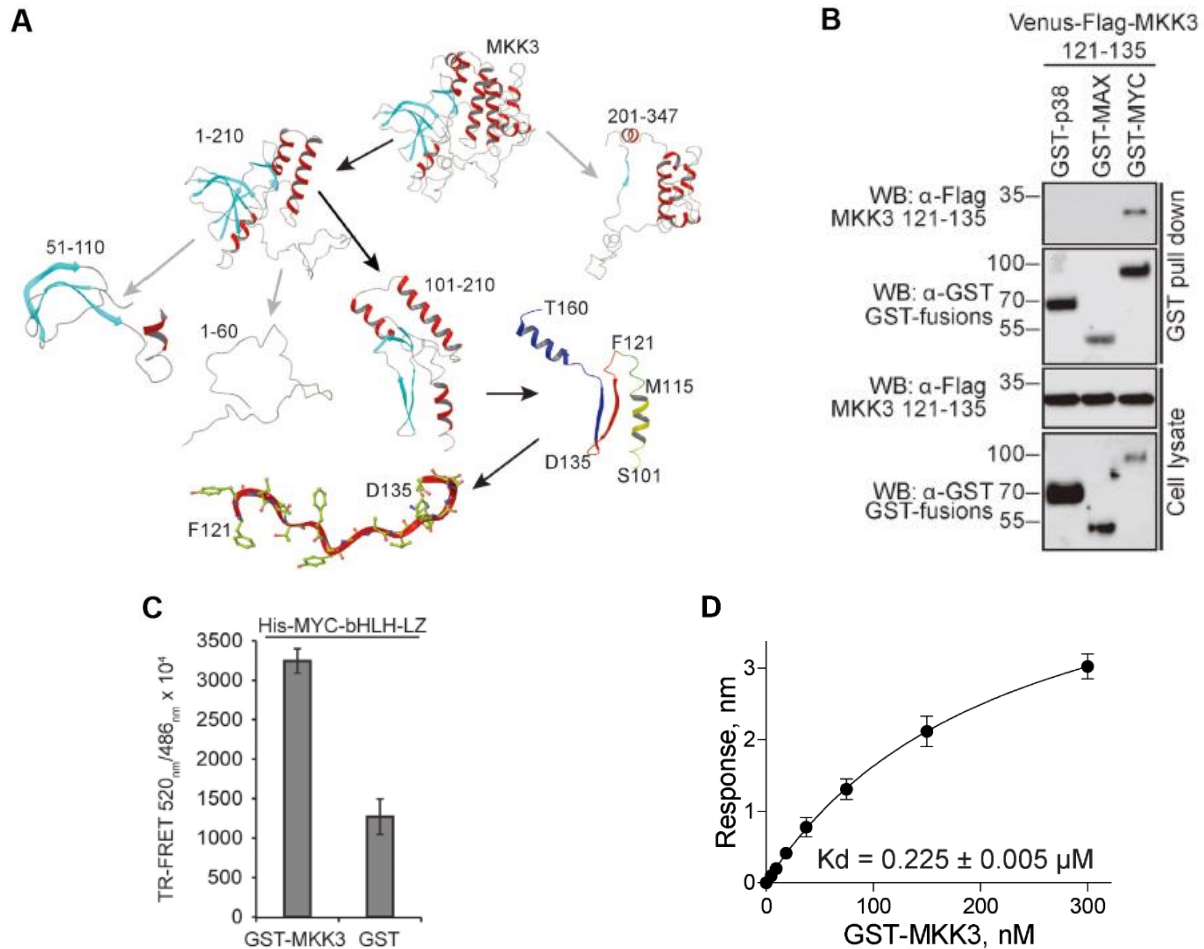


**Figure 5. MKK3/MYC PPI was validated in multiple orthogonal assays.** A) MKK3 interacts with MYC in reciprocal GST-pull down assays. The assay was performed in HEK293T cells expressing GST- and Venus-Flag-tagged MKK3 and MYC. GST and Flag-Venus alone served as negative controls<sup>31</sup>. B) Endogenous co-IP of MKK3 with MYC in breast cancer MCF7 cells. Mouse IgG was used as a negative control for the assay<sup>31</sup>. C) Endogenous co-IP of MYC with MKK3 in MCF7 cells<sup>31</sup>. D) MKK3 interacts with MYC in live MCF7 cells. This panel shows a representative image of MCF7 cells with green fluorescence produced by reconstituted Venus from overexpression of MKK3 conjugated with N-terminal part of Venus (NVen-MKK3) with MYC or p38 conjugated with Venus C-terminal (CVen) part of Venus protein but not for individually transfected proteins. Hoechst nuclei staining is shown in blue. The bars on the right side represent green fluorescence of reconstituted Venus detected in triplicate in MCF7 cells<sup>31</sup>.

## Interrogation of MKK3/MYC PPI Interface

After validating this novel protein-protein interaction, MKK3 and MYC truncations were generated in order to identify specific binding motifs in each binding partner. Biological assays, such as TR-FRET, GST pull-down, and Bio-Layer interferometry (BLI), together with computational molecular modeling, identified MYC basic-Helix-Loop-Helix (bHLH) domain (353-439) and MKK3 121-135, as the interaction domains (Fig. 6A-D).



Ivanov *et al.*, 2017

**Figure 6. Identification of binding-domains on MKK3 and MYC responsible for their interaction.** A) A computational model of MKK3 was utilized to guide the design of truncation fragments. MKK3 MYC-binding fragments are highlighted with black arrows<sup>31</sup>. B) Interaction of MKK3 121–135 peptide with MYC in a GST-pull down assay in HEK293T cells with p38 and MAX as controls<sup>31</sup>. C) MYC bHLH-LZ domain is sufficient for MKK3 binding in vitro. Recombinant GST-MKK3 and His-MYC-bHLH-LZ proteins were used in a TR-FRET assay. Recombinant GST protein was used as a negative control. TR-FRET signal was measured in triplicate<sup>31</sup>. D) The interaction between recombinant GST-MKK3 and His-MYC-bHLH-LZ was detected using the BLI assay. The maximum change in light interference in the association step was determined for indicated concentrations of GST-MKK3. A standard curve was plotted using one-site binding (hyperbola) nonlinear regression. The error bars indicate s.d. of three independent experiments<sup>31</sup>.

### **Functional Studies Indicate MKK3/MYC PPI as a Potential Therapeutic Target**

In the previous study, the function of MKK3/MYC PPI was investigated. The effect of MKK3-binding to MYC protein stability was tested through the cycloheximide (CHX) assay. After CHX is added to cells, protein synthesis will be inhibited. The longer the treatment time is, the more protein will degrade, and thus the less protein will remain. Compared to the Venus vector control, MKK3 and MKK3 121-135 overexpression led to slower rate of protein degradation, indicating that MKK3 stabilizes MYC protein (Fig 7A).

Furthermore, MYC transcriptional activity in cells with or without MKK3 overexpression was tested using the classical MYC reporter assay. When MKK3 or MKK3 121-135 was overexpressed in cells, MYC transcriptional activity was significantly upregulated in multiple cell lines (Fig. 7B).

Besides that MYC protein stability and transcriptional activity is upregulated upon its interaction with the Mitogen-Activated Protein Kinase Kinase 3 (MKK3)<sup>30-32</sup>, MKK3 level was also correlated with the expression of cell-cycle regulating MYC-target genes<sup>31</sup> (Fig. 7C). These observations suggested a new role for MKK3 as a novel regulator of MYC transcriptional program<sup>31</sup> (Fig. 7D).

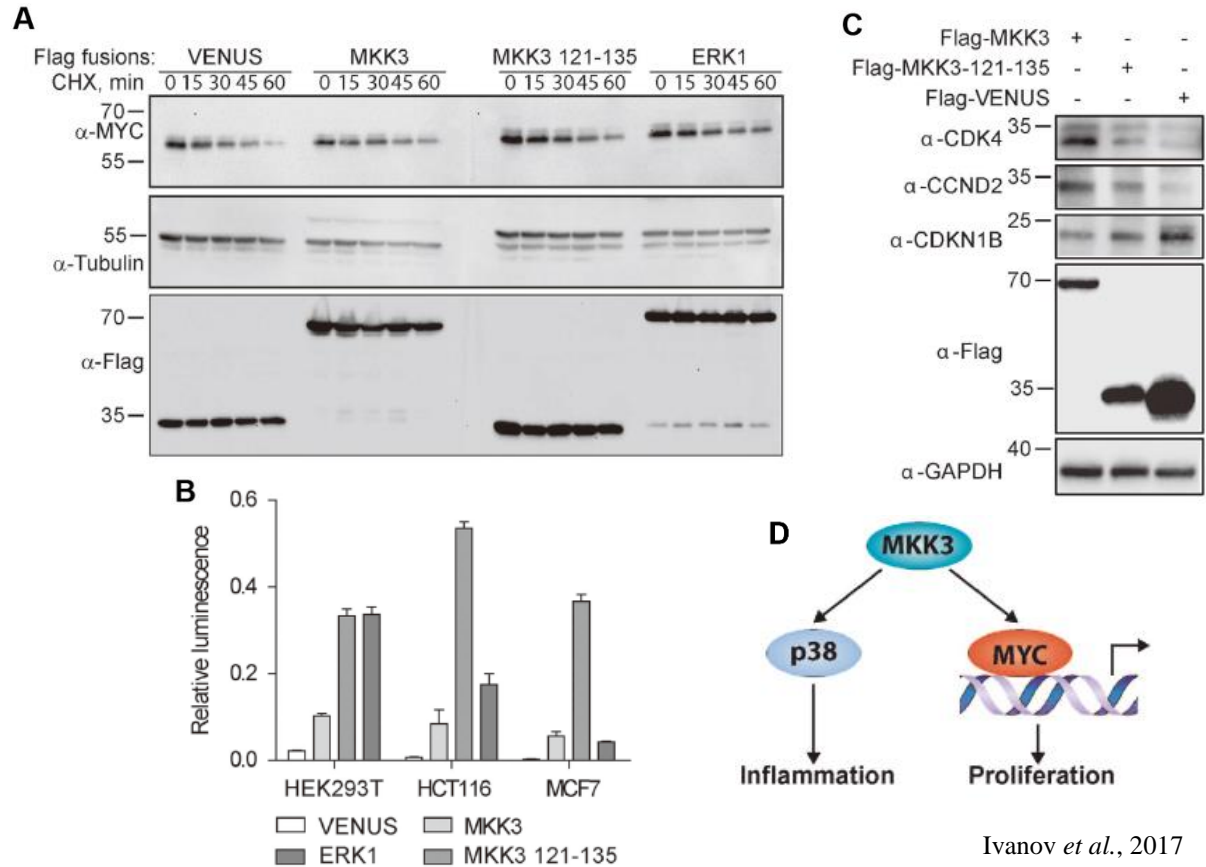


**Figure 7. MKK3 inhibits MYC degradation and upregulates its activity.** A) MKK3 and MKK3 121–135 MYC-binding peptide inhibit MYC degradation in HCT116 cells. HCT116 cells were transfected with Venus-Flag-MKK3, Venus-Flag-MKK3 121–135, Venus-Flag-ERK1 or Flag-Venus alone for 48 h and treated with 100 $\mu$ g/ml cycloheximide (CHX) for indicated times. Western blotting was performed to reveal the level of endogenous MYC. Tubulin was used as a control<sup>31</sup>. B) MKK3 and MKK3 121–135 enhance MYC transcriptional activity in HEK293T, HCT116 and MCF7 cells in a MYC luciferase reporter assay. The cells were co-transfected with Venus-Flag-MKK3, Venus-Flag-MKK3 121–135, or Flag-Venus, Firefly luciferase reporter plasmid containing four E-box sites, and Renilla luciferase used as a transfection efficiency control. The MYC transcriptional activity is expressed as the relative luminescence calculated as the ratio of luminescence produced by Firefly luciferase to the luminescence produced by Renilla luciferase<sup>31</sup>. C) MKK3 modulates MYC activity to control expression of cell cycle regulating genes. The level of CDK4, CCND2 and CDKN1B was determined by western blot analysis of HCT116 cells expressing Venus-Flag fusions of MKK3 and MKK3 121–135. Flag-Venus served as a background control. GAPDH was used as a loading control. Overexpression of both MKK3 and MKK3 121–135 correlate with increased levels of CDK4 and CCND2 and decreased levels of CDKN1B compared with the Venus control<sup>31</sup>. D) Working model. In addition to the established MKK3/p38 pathway, MKK3 may regulate MYC activity through a direct physical PPI<sup>31</sup>.

## Scope of the Thesis

In this study, we report the discovery of the first-in-class small molecule inhibitors and peptide antagonist for the MKK3/MYC interaction, as well as the potential regulatory mechanism between MAP Kinase signaling pathway and MYC transcriptional program. At the first stage, truncations from MYC bHLH domain were generated in order to identify a more specific MKK3-binding domain in MYC. MYC 370-413, termed PEP4, was demonstrated to be the shortest peptide sufficient for MKK3-binding. Multiple biological assays were performed to demonstrate that PEP4 can inhibit the binding between MKK3 and MYC. Overexpression of this 44-amino-acid peptide showed significant cell growth inhibition and cell death induction effect in multiple cancer cell lines. Together, these findings indicate that this interaction can be disrupted, and the disruption has tremendous antitumor effect. Therefore, small molecule chemical tools are in need to further probe this tumor promotive interaction. To identify small molecule MKK3/MYC PPI inhibitors, we have developed and applied a cell lysate-based time-resolved fluorescence energy transfer (TR-FRET) assay optimized for a 1536-well ultra-high-throughput (uHTS) format. The pilot screen of ~6,000 compounds from three small molecule compound libraries followed by a hit validation in a panel of orthogonal assays revealed the quinoline derivative SGI-1027 as the most potent MKK3/MYC PPI inhibitor ( $IC_{50} = 8 \mu M$ ). We showed that SGI-1027 suppresses MYC transcriptional activity and proliferation of a panel of MYC-dependent cell lines. Furthermore, SGI-1027 demonstrates a notable specificity against well-defined MKK3/p38 and MYC/MAX PPIs.

Besides the discovery and development of MKK3/MYC PPI inhibitors, we also aimed to investigate the mechanism for this crosstalk between MAP Kinase signaling pathway and MYC transcriptional program. The effect of overexpression of several MKK3 or MYC regulatory

proteins to this particular PPI was studied and results indicated that ASK1 might act as a switch for MKK3 to decide which downstream direction to go: activating the well-known p38 MAPK pro-inflammatory pathway, or activating oncogenic MYC transcriptional program. Moreover, we found that GSK3 $\beta$ , an essential MYC regulator which promotes MYC degradation by phosphorylation, is a potential novel binding partner of MKK3. When MKK3 is present, lower level of MYC/GSK3 $\beta$  interaction could be detected, indicating that MKK3 might enhance MYC stability by inhibiting its interaction with GSK3 $\beta$ . These completely new findings would provide a new scope and support for future investigation of MYC regulation mechanisms.

Together, this study provides a new approach to target MYC oncogenic activity through the disruption of its complex with MKK3, and builds a basis for further development of small molecule chemical probes to interrogate oncogenic pathways driven through MYC protein-protein interactions.

# **MATERIALS AND METHODS**

### *Reagents*

Tb cryptate-conjugated mouse monoclonal anti-Flag antibody (anti-Flag-Tb, #61FG2TLB) and d2-conjugated anti-GST antibody (anti-GST-d2, #61GSTDLB) were purchased from Cisbio Bioassays (Bedford, MA). Monoclonal ANTI-FLAG® M2-Peroxidase (HRP) antibody (#A8592, 1:2500 dilution), anti-Glutathione-S-Transferase (GST)-Peroxidase Conjugate antibody (#A7340, 1:2500 dilution), monoclonal Anti- $\beta$ -Actin antibody (#A5441, 1:5000 dilution), and protease inhibitor (#P8340) were purchased from Sigma-Aldrich. c-Myc (D84C12) Rabbit monoclonal antibody (#5605S, 1:1000 dilution) was purchased from Cell Signaling. Peroxidase AffiniPure Goat Anti-Rabbit IgG (H+L) secondary antibody (#111-035-003, 1:5000 dilution), and Peroxidase AffiniPure Goat Anti-Mouse IgG (H+L) secondary antibody (#115-035-003, 1:5000 dilution) were purchased from Jackson ImmunoResearch.

Polyethylenimine (PEI; Polysciences, Inc.), dissolved in sterile water at a concentration of 1 mg/mL, was used as transfection reagent for HEK293T cells. FuGENE® HD (Promega, #E2311) was used as transfection reagent for and HCT116 cells.

### *Cell Line and Culture Conditions*

Human embryonic kidney 293T cells (HEK293T; ATCC®, CRL-3216) and human colorectal carcinoma HCT116 cells (ATCC®, CCL-247) were cultured in Dulbecco's modified Eagle's medium (Corning, #10-013-CV) Cell culture medium was supplemented with 10% fetal bovine serum (ATLANTA biologicals, #S11550) and 100 IU/ mL penicillin in a humid environment with 5% CO<sub>2</sub> at 37C°.

### *DNA Constructs*

All GST-, VF-tagged human MKK3 and MYC plasmids for mammalian expression were generated using Gateway cloning technology (Invitrogen) as described previously<sup>31</sup>. pDONR223 vector, pDEST vectors for GST-tag and Venus-Flag-tag were purchased from Invitrogen. The DNA was purified using ZymoPURE® Plasmid Maxiprep Kit (Zymo Research; #D4203).

### *GST-pull down Assay*

HEK293T cells were co-transfected with GST- and Venus-Flag-tagged proteins, or empty vectors as negative controls. The proteins were expressed for 48h, lysed, and incubated at a low speed of rotation with Glutathione Sepharose® 4B beads (GE Healthcare, #17-0756-05) at 4 °C for 3 hours for regular pull-down assays. While for pull-down validations for compound hits revealed by pilot screening, cell lysate with overexpression of GST-tagged and VF-tagged proteins was first incubated with compounds for 30 minutes, and then beads were added and the mixture was further incubated for 75 minutes. After incubation, beads were washed three times with the 1% NP-40 lysis buffer, eluted by boiling in sodium dodecyl sulfate-polyacrylamide gel electrophoresis (SDS-PAGE) loading buffer, and analyzed by Western blotting.

### *Western Blot*

Proteins in sample buffer were separated by 10% SDS polyacrylamide gel electrophoresis (10% acrylamide gels) and were transferred to nitrocellulose filter membranes at 100 V for 2 h at 4 °C. After blocking the membranes in 5% nonfat dry milk in 1×TBST (20mM Tris-base, 150mM NaCl, and 0.05% Tween 20) for 30 minutes to 1 hour at room temperature, membranes were blotted with the indicated antibodies overnight at 4 °C. Membranes were washed by 1×TBST for three times,

5 minutes each time. SuperSignal West Pico PLUS Chemiluminescent Substrate (Thermo, #34580) and Dura Extended Duration Substrate (Thermo, #34076) were used for developing membranes.

#### *TR-FRET Measurements*

The FRET buffer used in all TR-FRET assays contains 20 mM Tris-HCl, pH 7.0, 50 mM NaCl, and 0.01% nonidet P-40 (NP-40). FRET signals were measured BMG Labtech PHERAstar FSX reader. Terbium was used as TR-FRET donor and excited at 337 nm laser. Venus or d2 served as TR-FRET acceptors for Tb/Venus and Tb/d2 pairs, respectively. When Venus served as an acceptor for Tb, the emissions for Tb and Venus were measured at 486 and 520 nm, respectively. When d2 served as acceptor for Tb, the emissions for Tb and d2 were measured at 615 and 665 nm, respectively. The delay time was set as 50 ms and total time of windows was 150 ms. All FRET signals were expressed as a TR-FRET ratio: F620nm/F655nm. For the cell lysis-based experiments the transfection efficiency was monitored based on the Venus fluorescence produced by Venus-tagged proteins.

#### *Development of MKK3/MYC TR-FRET Assay in a 384-Well HTS Format*

Based on results from optimization, the antibody combination of anti-GST-d2 and anti-Flag-Tb was selected for MKK3/MYC TR-FRET assay. Cell lysates were obtained from HEK293T cells co-transfected with VF-MYC and GST-MKK3 in 6-well plates (Greiner, #657160). Transfection was performed by mixing 1 $\mu$ g of GST-tagged plasmid and 1 $\mu$ g of VF-tagged plasmid with 6 $\mu$ L of PEI transfection reagent (plasmid (w): transfection reagent (w) = 1:3) and 100 $\mu$ L of cell culture medium. After vortex and centrifugation, the mixture was incubated under room temperature for 15 minutes, and then the entire volume was added to one well of six

well plate. After incubation for 48 hours, the cells were harvested and lysed with 1% NP-40 lysis buffer, 200 $\mu$ L per well, for 1 hour at 4°C, and then centrifuged at 14800 rpm for 10 minutes at 4°C. Supernatant was collected as cell lysate stock.

To determine the optimal dilution of cell lysate that can generate the highest FR-FRET signal, cell lysate titration was first performed in black solid bottom 384-well plates (Corning®, #3573). 20 $\mu$ L of cell lysate was serially diluted in FRET buffer and mixed with 5 $\mu$ L of anti-GST-d2 and 5 $\mu$ L anti-Flag-Tb antibody, diluted at 1:83 and 1:125 in FRET buffer, respectively, yielding 1:500 and 1:750 final dilutions, respectively. The plate was centrifuged at 1000 rpm for 2 minutes and incubated at room temperature for 2 hours. TR-FRET signal was then measured with BMG Labtech PHERAstar FSX reader. The laser excitation at 337nm and the emission at 615 and 665nm was used for Tb and d2 emission signals, respectively. FR-FRET signal was expressed as ratio:  $F_{665}/F_{615} \times 10^4$ .

#### *Miniaturization of the Assay into a 1,536-Well uHTS Format*

The TR-FRET assay for uHTS was performed in a black 1,536-well plate (Corning, #3724). The reaction mixture contained the optimal amount of GST-MKK3/VF-MYC co-expression lysate, anti-GST-d2 (1:500), and anti-Flag-Tb (1:750) antibodies. The reaction mixture was dispensed to black 1,536-well plates (5 $\mu$ L/well) using multiple-drop Combi dispenser (Thermo, #5840320). The VF-MYC lysate only without GST-MKK3 co-expression was used as background control. The TR-FRET signals were measured using BMG Labtech PHERAstar FSX plate reader.

### *Pilot Screening for Potential MKK3/MYC Inhibitors through uHTS in a 1536-Well Format*

To look for small molecule compounds that can potentially act as MKK3/MYC inhibitors, pilot screening was performed with the LOPAC, Spectrum, and Emory Enriched EEL libraries, containing 1280, 2000, and 2609 pharmacologically active compounds, respectively. As described before, 5 $\mu$ L of reaction mixture, containing cell lysate with GST-MKK3 and VF-MYC co-expressed, anti-GST-d2 antibody diluted at 1:500, and anti-Flag-Tb antibody diluted at 1:750, was dispensed into each well of the 1536-well black solid bottom plates. The library compounds were added using pintoole integrated with Beckman NX (Beckman Coulter, Brea, CA), giving a final compound concentration of 10 $\mu$ M. After centrifugation and incubation at room temperature for 2 hours, TR-FRET signals were measured using BMG Labtech PHERAstar FSX plate reader.

### *Dose-Response TR-FRET Validation for Compound Hits*

To validate the hits revealed by pilot screening, compounds' effects to MKK3/MYC PPI were tested in a dose-dependent manner in 384-well black solid bottom plate. For the HEK293T cells expressing GST-MKK3 and VF-MYC were lysed as described above. 40  $\mu$ g/mL total protein was used in the assay. For the assay with recombinant purified proteins, GST-MKK3 and His-tagged MYC Helix-Loop-Helix domain were purified as described previously<sup>31</sup>. The final concentrations of GST-MKK3 and His-MYC-HLH were 10nM and 1  $\mu$ M, respectively. The reaction mixture (30  $\mu$ M/well) contained 20 $\mu$ L of the lysate or purified protein mixture combined with anti-GST-d2 antibody, anti-Flag-Tb antibody, and compounds at 0 to 50  $\mu$ M concentration range. The reaction mixtures were incubated at room temperature for 2 hours, and TR-FRET signals were measured using BMG Labtech PHERAstar FSX plate reader.

### *Data analysis*

All experiments were repeated at least three times. The data quantification was performed using the GraphPad Prism software. (GraphPad Software, Inc., La Jolla, CA, USA)

### *MYC reporter assay*

The MYC transcription activity was measured using MYC reporter assay as described previously<sup>31</sup>. Colon cancer HCT116 cells grown in 6-well plates were transfected with Venus-Flag-MKK3, or Venus-Flag vector along with the Firefly luciferase reporter plasmid containing three MYC EBOX sites: GCCACGTGGCCACGTGGCCACGTGGC. The EBOX mutated that cannot be recognized by MYC (GCCTCGAGGCCTCGAGGCCTCGAGGC) was used as a negative control. Renilla luciferase expression vector served as a normalization control for protein expression. SGI-1027 compound was added to cells 36 hours after transfection, and cells were further incubated for 12 hours. Then, cells were harvested, and transferred to a 384-well plate (20  $\mu$ L per well). MYC reporter assay was performed using Nano-Glo Dual-Luciferase Reporter Assay System (Promega, Madison, WI, USA, cat # N1610) following the manufacturer's instructions. The normalized luminescence was calculated as a ratio of luminescence of Firefly luciferase to the luminescence of Renilla luciferase. The MYC activity was represented as a fold over control calculated as ratio of the relative luminescence calculated for cells transfected with the EBOX wild type reporter to the relative luminescence calculated for cells transfected with EBOX mutant reporter plasmid.

### *Computational modeling*

First, the ICM Pro software was utilized to evaluate potential binding sites for SGI-1027 on the MKK3 surface. The grid box of 78Å x 87Å x 81Å was generated around MKK3 to cover the whole protein structure. Molecular docking was performed using the following parameters: score version: 2005, solvation electrostatic method: generalized Born, flexible ring sampling level: 2, charge groups: auto, docking effort: 10, maximum number of conformations 1,000,000. The binding poses were evaluated in terms of the ICM Score. In its most favorable pose, SGI-1027 appeared in proximity to MKK3 121-135 residues, and was characterized by the Score of -38.46. Then, this model was further validated using the Schrodinger Glide software. The LigPrep program was used to generate a set of SGI-1027 initial conformations. The grid box with the sides of 20Å was defined around the SGI-1027 docked by ICM Pro and SGI-1027 was redocked using the Glide XP precision mode. The most favorable binding mode selected based on the XP GScore was in excellent agreement with the results obtained with the ICM Pro docking. The model was further refined with 100 ns molecular dynamics (MD) simulation using Desmond software. The MD simulation was performed in the orthorhombic water box using constant-temperature, constant-pressure (NPT) ensemble class ( $T = 300.0\text{K}$  and  $p = 1.01325\text{ bar}$ ). The Nose-Hoover chain thermostat method was used. The average MKK3-SGI-1027 model was calculated based on the last 100ps of simulation. The SGI-1027 binding energy ( $dG_{\text{Bind}} = -80.836$ ) was evaluated using the molecular mechanics generalized Born and surface area continuum method (MM-GBSA) implemented in the Schrodinger Prime software.

# RESULTS

### Shorter truncations were designed and generated from MYC bHLH domain

Previously, through the computational and biochemical studies our group have determined MYC Helix-Loop-Helix (HLH) domain (MYC 353-439) as the main MYC binding for MKK3 surface<sup>31</sup>. To further characterize the MKK3/MYC PPI interface, several peptide fragments derived from MYC HLH were designed (Fig. 8A). Namely, MYC 353-387, MYC 387-439, MYC 370-413, and MYC 362-381 were generated. The peptides were cloned into Venus-Flag-tagged expression vectors using Gateway cloning technology (Invitrogen). All constructs were verified through DNA gel electrophoresis and sequencing. (Fig. 8B). Their interaction with GST-MKK3 was tested in GST pull down assay as described in Methods. Based on the Western blotting, the strongest interactions were observed for the MYC HLH as well as for MYC 387-439 and MYC 370-413 located in the middle region of the MYC HLH domain (Fig. 8C). In contrast, no interaction was observed for GST-MKK3 with MYC 353-387, MYC 362-381, nor Venus vector used as a negative control for the assay.

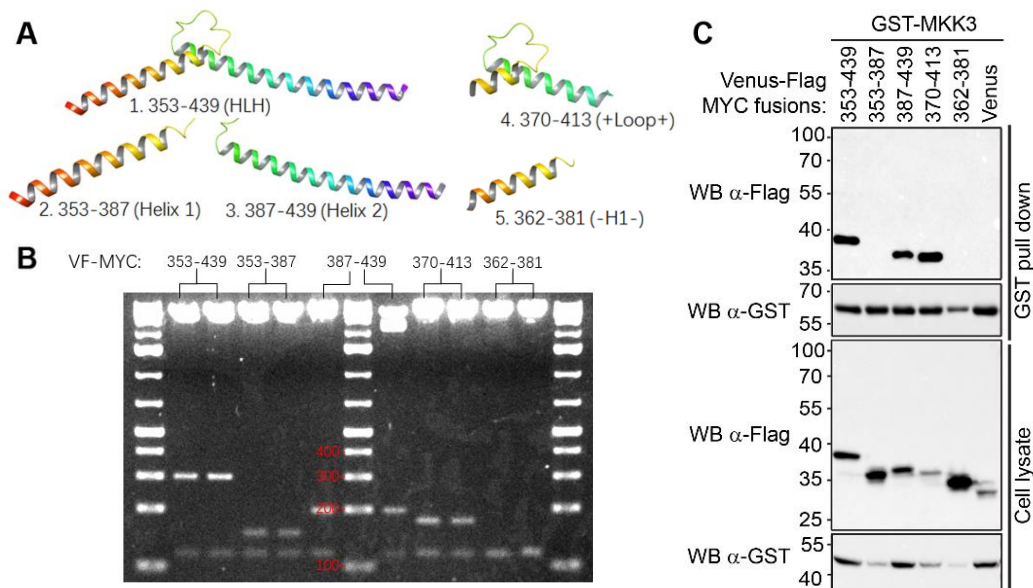


**Figure 8. Identification of MKK3-binding site on MYC HLH-domain.** A) Crystal structure of truncations designed from the MYC HLH-domain; B) The sizes of Venus-Flag fusions of MYC fragments were verified through DNA gel electrophoresis. C) MYC 353-439, 387-439, and 370-413 fragments interact with GST-MKK3 in GST pull down assay. The assay was performed using the HEK293T cells co-expressing GST-MKK3 and Venus-Flag fusions of MYC fragments. Venus-Flag vector was used as a negative control.

### **MKK3/MYC PPI can be disrupted by inhibitory peptides**

Since MYC 370-413 was identified as a shortest MKK3-binding peptide, we tested whether MYC 370-413 is also sufficient to disrupt the interaction between GST-MKK3 and MYC in GST pull down assay. We found that indeed, co-expression of GST-MKK3 with VF- MYC 370-413 suppressed the binding of endogenous MYC to GST-MKK3 in HEK293T cells comparing to the non-binding VF-MYC 353-837 or Venus vector control (Fig. 9A).

MYC HLH domain is known for its critical role in dimerization with MYC major binding partner MAX to bind the DNA. Since MYC 370-413 was derived from MYC HLH, we tested its effects on MYC/MAX PPI. We found that in contrast to its inhibitory effect on the MKK3/MYC PPI, MYC 370-413 does not significantly decrease MYC/MAX interaction in GST pull down assay (Fig. 9B). This result is in agreement with the crystallographic data available for MYC/MAX complex <sup>26</sup>. It has been shown that MYC binds to MAX through the Leucine Zipper motif, and MYC Arg424 and Arg423 are essential for MYC/MAX heterodimerization <sup>26</sup>. PEP4 (MYC 370-413) does not include these residues and thus is not expected to form a stable complex with MAX. Furthermore, we did not observe a binding of VF-MYC 370-413 to the major MKK3 substrate, p38, nor to a well-established regulator of MYC GSK3 $\beta$  (Fig. 9C).

### **Overexpression of MKK3/MYC inhibitory peptide correlates with anti-tumor effects**

Since MYC amplification is strongly correlated with tumorigenesis, inhibition of MYC activation could lead to significant anti-tumor effect. Knowing that MKK3 can serve as a MYC activator through enhancing MYC transcriptional activity and protein stability, we hypothesized that the peptide antagonist might be able to decrease MYC activity by blocking the interface for MKK3/MYC PPI, and, therefore, lead to inhibitory effects in cancer cells.

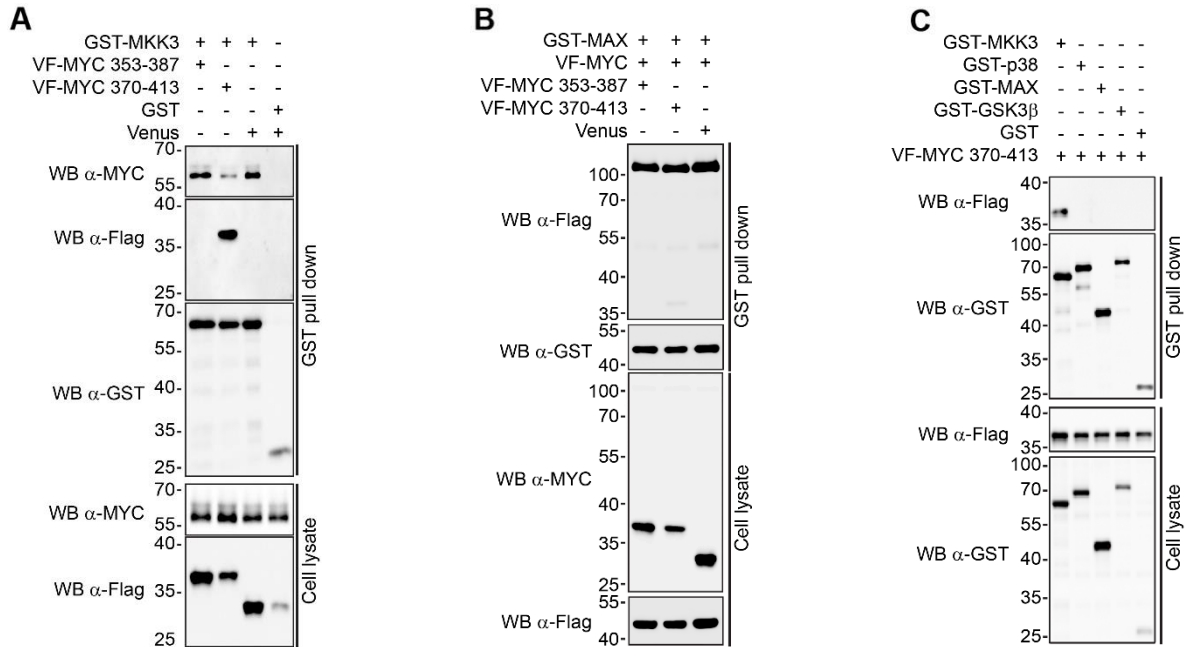


**Figure 9. MYC 370-413 selectively inhibits the interaction between MKK3 and MYC.** A) Venus-Flag (VF)-MYC 370-413 inhibits the interaction of endogenous MYC with GST-MKK3 in GST pull down assay. The assay was performed using the HEK293T cells co-expressing GST-MKK3 with VF-MYC 370-413. Non-binding VF-MYC 353-387 fragment and Venus-Flag vectors served as negative and vehicle controls, respectively. B) VF-MYC 370-413 peptide does not interfere with GST-MAX/VF-MYC PPI comparing to VF-MYC 353-387 and Venus-Flag vector controls in GST pull down assay performed in HEK293T cells. C) VF-MYC 370-412 demonstrates higher affinity for GST-MKK3 comparing to GST-p38, GST-MAX, and GST-GSK3 $\beta$  in GST pull down assay performed in HEK293T cells. GST vector served as a negative control.

To test the effect of inhibitory peptide to cancer cells, VF-PEP4 was first overexpressed in H1299 lung cancer cells. Non-binding peptide MYC 353-387 (PEP2) and Venus-Flag vector were used as negative controls. Cell proliferation was monitored using the IncuCyte live-cell analysis system. The number of green cells, which were expressing the peptides, was counted, and the results demonstrates that the proliferation rate of cells expressing PEP4 is significantly slower than those of cells expressing PEP2 or Venus-Flag vector (Fig. 10A). In order to improve the efficiency of peptide overexpression, lentiviral transduction particles for VF-PEP4 and Venus vector were generated. Transduction efficiency of the lentivirus was tested in a panel of cancer cell lines, and the highest efficiency was observed in LN229 glioblastoma cells, as almost all cells expressed the peptide after transduction (Fig. 10B). 48 hours after transduction, LN229 cells were re-seeded into

96-well plate and green cell proliferation was monitored in real time with the IncuCyte system. Compared to Venus vector, PEP4 significantly inhibits proliferation of LN229 cells (Fig. 10C). In an independent experiment, the effect of PEP4 to cell death was tested, and the number of dead LN229 cells, expressing either PEP4 or Venus, was measured based on the red Propidium Iodide staining (Fig. 10D). The percentage of red cells in the peptide group was about three times higher than that in the vector group (Fig. 10E), indicating that PEP4 induces cell death in LN229 cells.

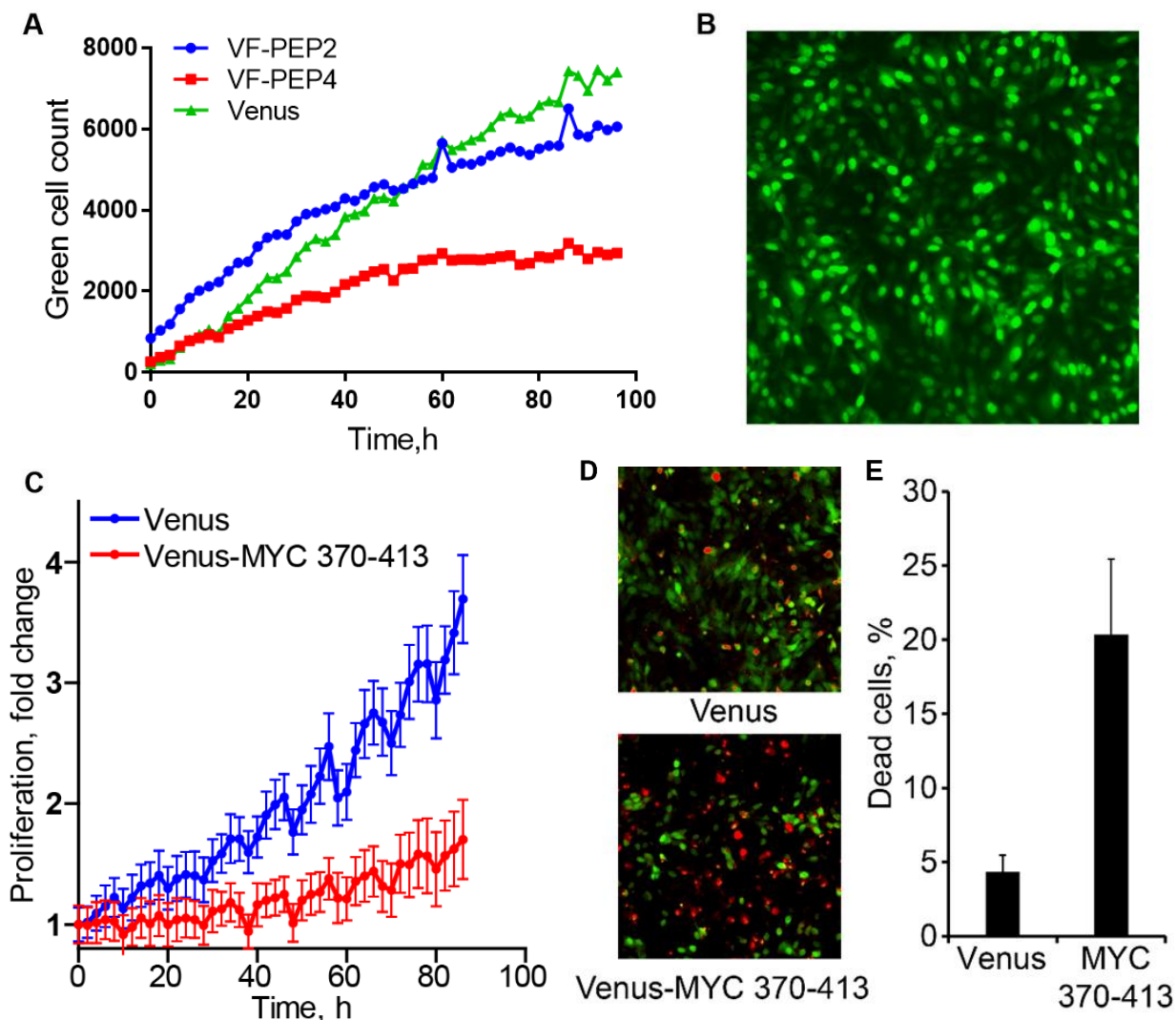


**Figure 10. Overexpression of peptide antagonist correlates with anti-tumor effects in cancer cells.** A) H1299 cells overexpressing PEP4 proliferate at a slower rate compared to those overexpressing non-binding peptide and Venus vector. B) Lentiviral transduction particles showed high efficiency in LN229 cells. C) LN229 cells overexpressing PEP4 proliferate at a slower rate compared to those overexpressing Venus vector. D) Propidium Iodide labeled dead LN229 cells as red. E) Quantification of dead LN229 cells showed that PEP4 induces cell death in LN229 cells.

## Further narrow-down of MKK3-binding site on MYC

Knowing that the 44-amino-acid MYC fragment 370-413 is sufficient for MKK3 binding, we further designed and generated shorter truncations based on previous data. The first short peptide generated was MYC 370-399, named PEP4S. The binding between Venus-Flag-tagged PEP4S and GST-MKK3 was tested in a GST-pull down assay. However, the result indicated that after removing the last 14 amino acids from PEP4, the 30-amino-acid PEP4S is no longer able to bind with MKK3 (Fig. 11A). Later, MYC 380-413 (PEP7), MYC 380-406 (PEP8), and MYC 370-406 (PEP9) were generated (Fig. 11B). GST pull-down assay revealed that all three peptides can bind to MKK3, while PEP8 and PEP9 can significantly inhibit the interaction between MKK3 and full-length MYC (Fig. 11C).

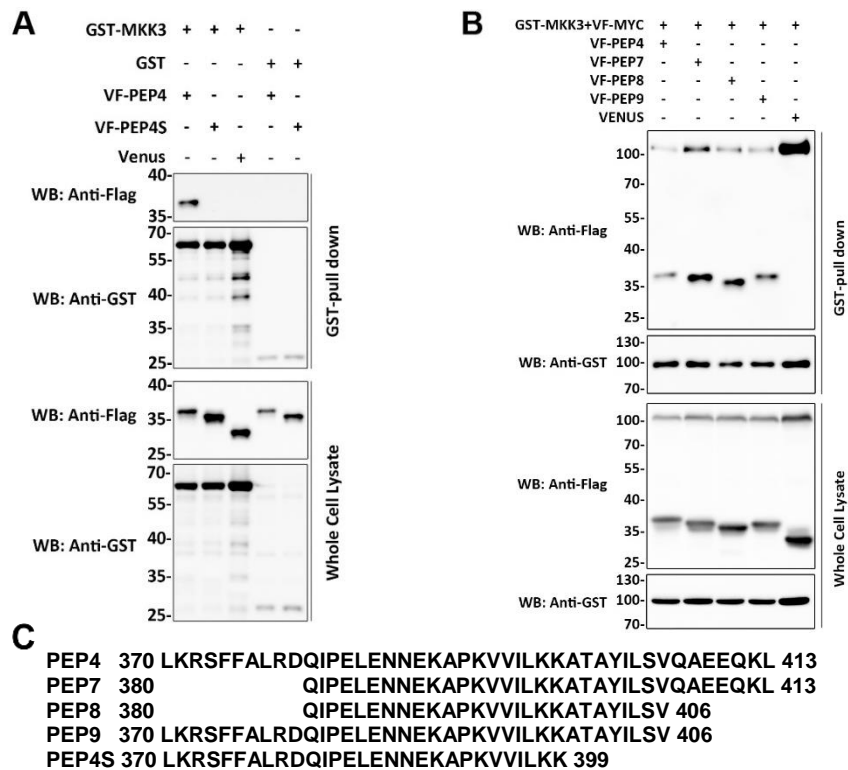


**Figure 11. MKK3-binding domain on MYC narrowed down to MYC 380-406.** A) VF-PEP4S does not bind to GST-MKK3 in GST pull-down assay. The assay was performed using the HEK293T cells co-expressing GST-MKK3 with VF-MYC 370-399. VF-PEP4 and Venus vector were used as positive and negative controls, respectively. B) Sequences of shorter peptides generated from PEP4. C) VF-PEP8 and VF-PEP9 can inhibit the interaction of VF-MYC with GST-MKK3 in GST pull down assay. The assay was performed using the HEK293T cells co-expressing GST-MKK3, VF-MYC and VF-tagged peptides. VF-PEP4 and Venus vector were used as positive and negative controls, respectively.

Together, these data have demonstrated not only that MYC 370-406 is the smallest MKK3-binding domain on MYC known to date, but also that MKK3/MYC PPI interface can be disrupted by peptide antagonist, and the disruption leads to significant decrease of cell proliferation and induction of cell death, which provided a basis to discover small molecule inhibitors for MKK3/MYC PPI.

### **Development of the ultra-high-throughput screening assay for MKK3/MYC PPI inhibitors**

To discover small molecule MKK3/MYC PPI inhibitors, the HTS TR-FRET cell lysate-based assay was developed to detect MKK3/MYC interaction directly from the cell lysates. This lysate-based approach has several advantages over conventional HTS assays with recombinant purified proteins. For example, the use of lysates of cells co-expressing the binding proteins allows to detect the PPIs under physiological conditions, including post-translational modifications. It also does not require protein purification steps that can be problematic and time consuming, especially for disordered nuclear proteins such as MYC.

Previously, we successfully used the lysate-based TR-FRET assay to detect different MKK3 PPIs, including MKK3/MYC interaction in mammalian cell lysates using the Venus tag as a TR-FRET signal acceptor and GST-Tb conjugated antibody as the TR-FRET donor<sup>31</sup>. On the other hand, we have shown that detection of MYC PPIs can be improved by using GST-d2/Flag-Tb pair of fluorophores<sup>33</sup>. Indeed, the TR-FRET signal detected for GST-MKK3/VF-MYC PPI using the GST-d2/Flag-Tb pair was 2-times stronger comparing to GST-Tb/Venus pair (Fig. 12A) and provided more than five-fold signal to background assay window. Furthermore, GST-d2/Flag-Tb fluorophore combination provides a TR-FRET signal that is stable for at least 48 hours after the addition of antibodies (Fig. 12B) and demonstrates a tolerance to up to 30% DMSO (Fig. 12C).

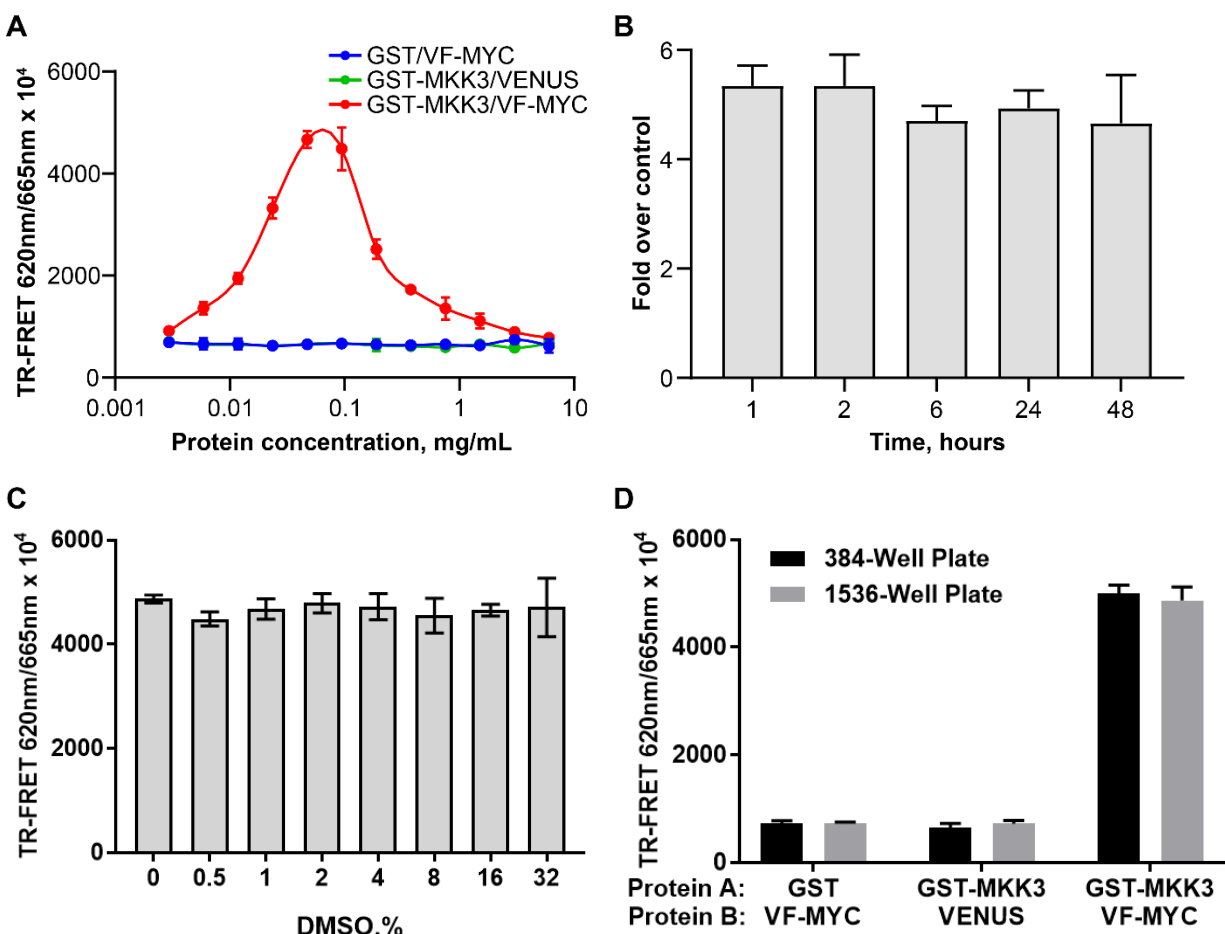


**Figure 12. Evaluation of the MKK3/MYC PPI TR-FRET assay.** A) GST-d2 and Flag-Tb fluorophore pair allows a 5-fold over control TR-FRET assay window in 384-well plate format; B) Temporal stability of TR-FRET signal. The TR-FRET signal was measured in time course of 48 h; C) The TR-FRET signal is stable in the presence of increasing amount of DMSO. D) The TR-FRET assay was miniaturized into a 1,536-well uHTS format, without significant difference between the TR-FRET signals detected from 384-well plates.

Therefore, GST-d2/Flag-Tb fluorophore combination was used for the HTS assay. To further improve the time and cost efficiency of the assay, the assay was miniaturized into a 1,536-well uHTS format. The same GST-MKK3/VF-MYC reaction mixture was added to 384-well (30 $\mu$ L/well) and 1,536-well plates (5 $\mu$ L/well), and the TR-FRET signal was measured and compared. As shown in Fig. 12D, we did not observe significant difference between the TR-FRET signals detected from 1,536-well and 384-well plates with more than 4-fold over control ratios in

both plate formats. Together, the optimized assay parameters allowed me to perform the pilot screening for MKK3/MYC PPI inhibitors in the 1536-well uHTS format.

### **The uHTS screening for MKK3/MYC PPI inhibitors**

To discover small molecule inhibitors of the MKK3/MYC PPI, the uHTS TR-FRET assay was performed using the SPECTRUM library (MicroSource, 2000 compounds), Library of Pharmacologically Active Compounds (LOPAC, Sigma-Aldrich, 1,260 compounds) and our in-house Emory Enriched Bioactive Library (EEBL) collection of 2,036 compounds. The EEBL library is enriched in pharmacologically active compounds with known biological and pharmacological activities and contains 1,018 FDA approved drugs. Recently, the library was successfully used to discover new IAP inhibitors as the immune enhancers<sup>34</sup>.

The assay was performed with the final compound concentration of 10  $\mu$ M in a 1,536-well uHTS format.  $Z'$  and Signal/Background (S/B) ratio were calculated for each plate. The  $Z'$  factors were  $> 0.7$  (Fig. 13A) and S/B was  $> 6$  (Fig. 13B) across five 1,536-well plates, demonstrating an excellent assay performance. The inhibitory effects of compounds were calculated in terms of the percent of inhibition compared to the DMSO control. The overall distribution of the percent of inhibition values is shown in Fig. 13C. Analysis of fluorescence intensity allowed to identify ~10% of compounds as fluorescent and potentially interfering with the TR-FRET assay (Fig. 13D). Compounds that demonstrated at least 20%-fold-change in fluorescence intensity comparing to DMSO control were eliminated from further analysis. After elimination of color quenching compounds, a total of 6 molecules have been identified with a hit cutoff of 30% inhibition: N-[4-[(2-Amino-6-methylpyrimidin-4-yl)amino]phenyl]-4-(quinolin-4-ylamino)benzamide (SGI-1027, 37% inhibition), 5-[(3-carboxy-4-hydroxyphenyl)-(3-carboxy-4-oxocyclohexa-2,5-dien-1-

ylidene)methyl]-2-hydroxybenzoic acid (Aurintricarboxylic acid or ATA, 58% inhibition), [2,6-di(propan-2-yl)phenyl] ~*(N)*-[2-[2,4,6-tri(propan-2-yl)phenyl]acetyl]sulfamate, (Avasimibe, 48% inhibition), and (-)-1,1',6,6',7,7'-Hexahydroxy-3,3'-dimethyl-5,5'-bis(1-methylethyl)-[2,2'-binaphthalene]-8,8'-dicarboxaldehyde (AT101, 31% inhibition) as well as Cisplatin and Sodium nitroferricyanide that showed 55% inhibition.

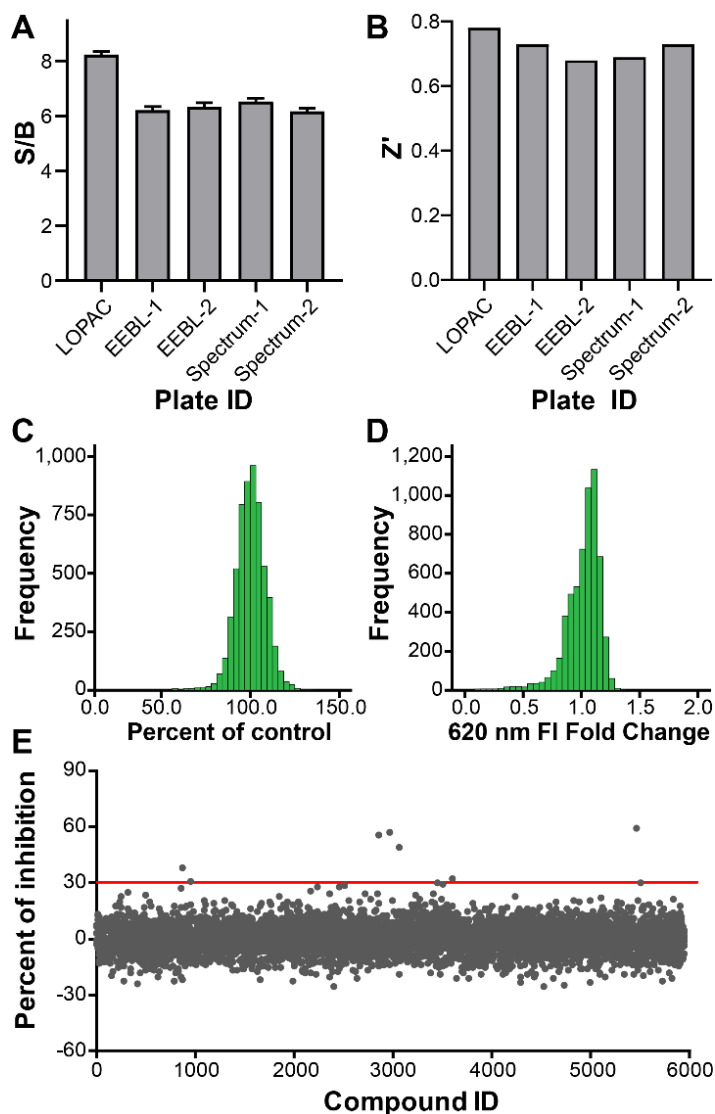


**Figure 13. Pilot uHTS screening for MKK3/MYC PPI inhibitors.** A) Each compound plate used in the uHTS assay demonstrated at least 6-fold difference between the signal and background (S/B). B)  $Z' > 0.7$  were determined for each compound plate used in the uHTS assay. C) Distribution of percent of inhibition determined in the uHTS TR-FRET-based screening. D) Distribution of compound fluorescence signal indicate that majority of the screened compounds did not interfere with the TR-FRET assay. Compounds that demonstrated at least 20%-fold change in fluorescence signal comparing to DMSO. E) The uHTS with the LOPAC, Spectrum, and EEBL libraries revealed five primary hits with more than 30% inhibition.

### **Validation of SGI-1027 as the disruptor of MKK3/MYC PPI**

Cisplatin and sodium nitroferricyanide are small inorganic molecules with broad spectrum of pharmacological activity and limited potential for further development as chemical probes. Therefore, these compounds were excluded from the further investigation. In contrast, SGI-1027, Avasimibe, ATA, and AT101 were selected for the validation in a dose-response (DR) TR-FRET assay (Fig. 14A-D). AT101 did not demonstrate detectable inhibition of MKK3/MYC PPI in the DR tests performed using 0 – 100  $\mu$ M compound concentrations. In contrast, the  $IC_{50}$  values of 8.46  $\mu$ M, 14.06  $\mu$ M, and 63.88  $\mu$ M were determined for SGI-1027, ATA, and Avasimibe, respectively.

Since SGI-1027 showed the highest potency as an MKK3/MYC PPI inhibitor in the DR TR-FRET assay, later, this compound was picked as the most promising lead. To validate the on-target effect of SGI-1027 on MKK3/MYC PPI, this compound was tested in TR-FRET assay using recombinant purified MKK3 and MYC proteins, instead of cell lysate with overexpressed GST-MKK3 and VF-MYC. Previously, through the structural modeling and biochemical studies, we have shown that MYC HLH domain is responsible for its binding to MKK3<sup>31</sup>. To determine whether SGI-1027 can interfere with the MKK3/MYC HLH binding, purified GST-MKK3 and His-tagged MYC-HLH were subjected in the TR-FRET assay. As shown in Fig. 15A, SGI-1027 can inhibit the interaction between GST-MKK3 and His-tagged MYC-HLH with the  $IC_{50} = 9.67 \pm 1.06 \mu$ M. These results are in excellent agreement with the cell lysate-based TR-FRET assay ( $IC_{50} = 8.46 \pm 1.53 \mu$ M) and support the direct effect of SGI-1027 on the interaction between MKK3 and MYC.

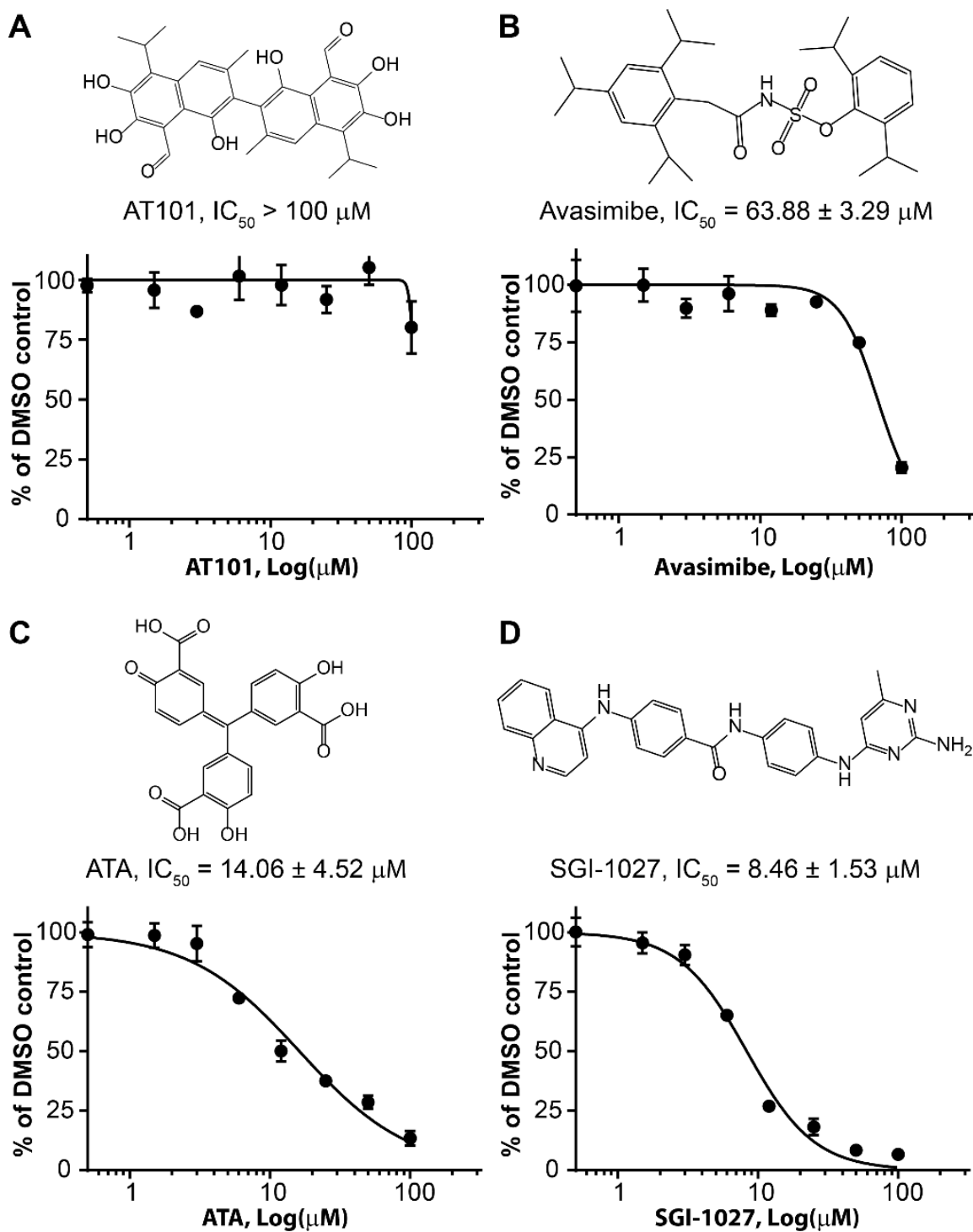


**Figure 14. Dose-response validation of primary hits detected in uHTS assay.** TR-FRET assay was performed for the lysates of HEK293T cells overexpressing GST-MKK3 and VF-MYC. The lysates were incubated for 2h with A) AT101, B) Avasimibe, C) ATA, or D) SGI-1027 in 384-well plates. DMSO was used as a vehicle control. The percent of control was calculated as a ratio of TR-FRET signal detected in a presence of compound to the TR-FRET signal obtained for the DMSO control. The average  $IC_{50}$  value was calculated based on three independent experiments.

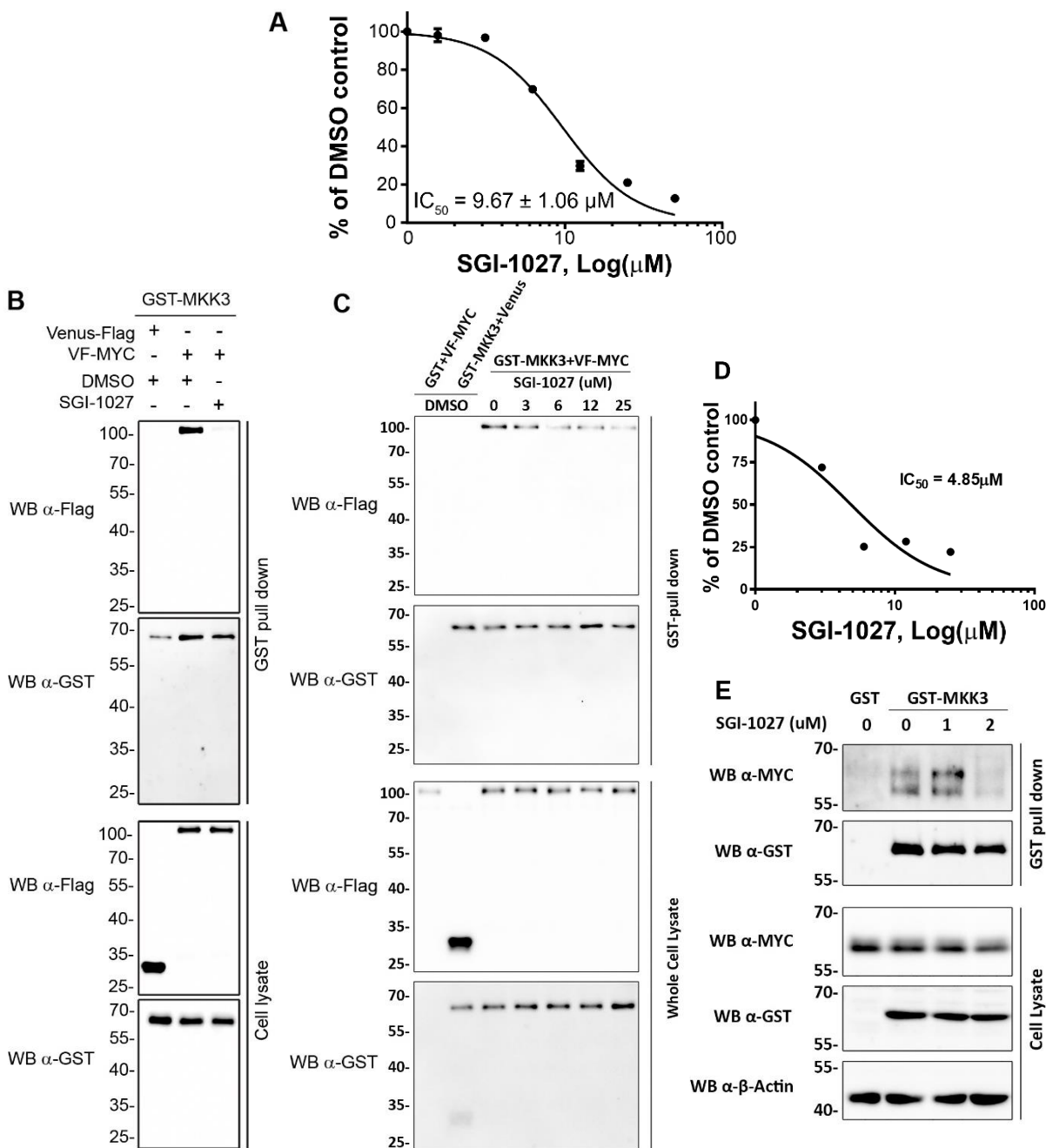


**Figure 15. Orthogonal validations of SGI-1027 as MKK3/MYC PPI inhibitor.** A) SGI-1027 inhibits the interaction between purified recombinant GST-MKK3 and MYC Helix-Loop-Helix domain in TR-FRET assay. Percentage of inhibition was calculated for each compound compared to DMSO control. B) SGI-1027 inhibits MKK3/MYC PPI in GST pull-down assay. GST-MKK3 and VF-MYC were co-expressed in HEK293T cells. The cell lysate was treated with 50  $\mu$ M SGI-1027. DMSO was used as a negative control. Venus vector served as negative control for the assay. B) SGI-1027 inhibits MKK3/MYC PPI in a dose-dependent manner in GST pull-down assay. DMSO was used as a negative control. GST and Venus vectors served as negative controls for the assay. C) Quantification for dose-response GST pull-down validation of SGI-1027.  $IC_{50}=4.85\mu$ M. D) SGI-1027 significantly inhibits the binding between GST-MKK3 and endogenous MYC at a concentration of 2 $\mu$ M in a semi-endogenous pull-down assay. GST-MKK3 was overexpressed in HCT116 colon cancer cells. 36-hours after transfection, the cells were treated with SGI-1027 and incubated in a humid environment with 5%  $CO_2$  at 37 $^{\circ}C$  for 12 hours. DMSO was used as a negative control. GST vector served as negative control for the assay.

Besides the TR-FRET system, the inhibitory effect of SGI-1027 on MKK3/MYC PPI was further validated in the orthogonal GST pull-down system. The compound was first tested in single-dose GST pull-down assay, which demonstrated that at a high concentration of 50  $\mu\text{M}$ , SGI-1027 leads to almost complete inhibition of MKK3/MYC PPI (Fig. 15B). Then dose-response GST pull-down assay was performed and  $\text{IC}_{50}$  was calculated after gel quantification (Fig. 15C-D). The  $\text{IC}_{50}=4.85 \mu\text{M}$  is in high agreement with the cell lysate-based TR-FRET assay ( $\text{IC}_{50} = 8.46 \pm 1.53 \mu\text{M}$ ) and the purified-protein-based TR-FRET assay ( $\text{IC}_{50} = 9.67 \pm 1.06 \mu\text{M}$ ). Furthermore, SGI-1027 was also validated to be able to significantly inhibit the interaction between overexpressed GST-MKK3 and endogenous MYC at 2  $\mu\text{M}$  (Fig. 15E). In conclusion, SGI-1027 has been validated as a promising MKK3/MYC PPI inhibitor in multiple orthogonal assays, with  $\text{IC}_{50}$  lower than 10  $\mu\text{M}$ .

### **SGI-1027 shows significant MKK3/MYC PPI selectivity**

To determine the specificity of SGI-1027 as the MKK3/MYC PPI inhibitor, we tested its effects on other related PPIs. First, we tested if SGI-1027 can disrupt the PPIs between major MKK3 and MYC binding partners p38 and MAX, respectively. While we have confirmed the inhibitory effect of SGI-1027 on MKK3/MYC PPI in the orthogonal GST pull down assay, we did not observe a significant suppression of MKK3-p38 or MYC-MAX PPIs by SGI-1027 at up to 50  $\mu\text{M}$  concentration (Fig. 16A-B). Previously our group have shown that besides p38 and MYC, MKK3 can interact with several other proteins, including Aurora kinase A (AURKA), the Ser/Thr kinase 11 (STK11), cyclin-dependent kinase 4 (CDK4), the autophagy regulator, Beclin 1; the angiogenesis modulator hypoxia-inducible factor 1-beta, Hippo signaling regulatory protein RASSF1, and several membrane-associated growth factor receptors including Ephrin type-A

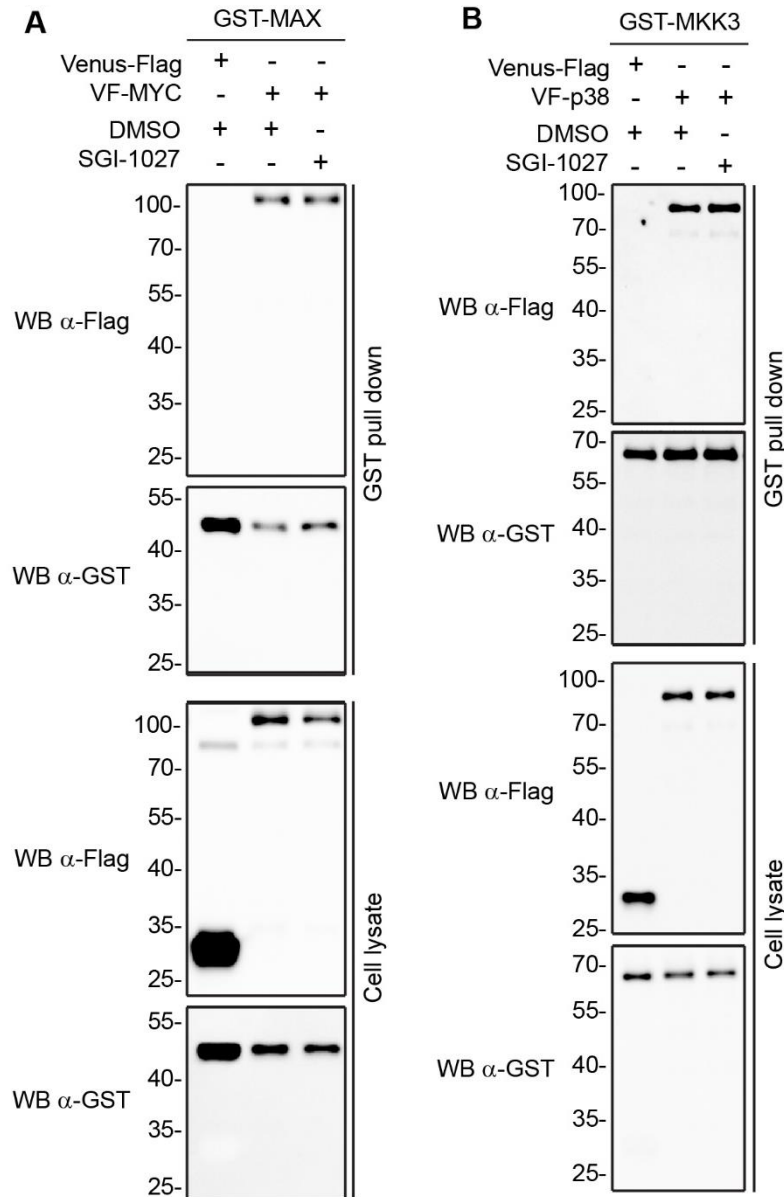


**Figure 16. SGI-1027 does not disrupt the PPIs between major MKK3 and MYC binding partners.** A) SGI-1027 does not inhibit the interaction between GST-MAX and VF-MYC at 50  $\mu$ M in GST pull-down assay. DMSO was used as a negative control. Venus vector served as negative control for the assay. B) SGI-1027 does not inhibit the interaction between GST-MKK3 and VF-p38 at 50  $\mu$ M in GST pull-down assay. DMSO was used as a negative control. Venus vector served as negative control for the assay.

receptor 2 (EPHA2), fibroblast growth factor receptor 4 (FGFR4), and platelet-derived growth factor receptor alpha (PDGFRA) (Fig. 4). The effects of SGI-1027 on these MKK3 PPIs were tested in the TR-FRET assay in parallel with MKK3/MYC interaction (Fig. 17 A-B). As shown in Fig. 17C, the treatment of cell lysates co-expressing GST-MKK3 and VF-MYC with 12  $\mu$ M SGI-

1027 resulted in at least 70% inhibition of the PPI comparing to the DMSO control. In contrast, the compound effects on all

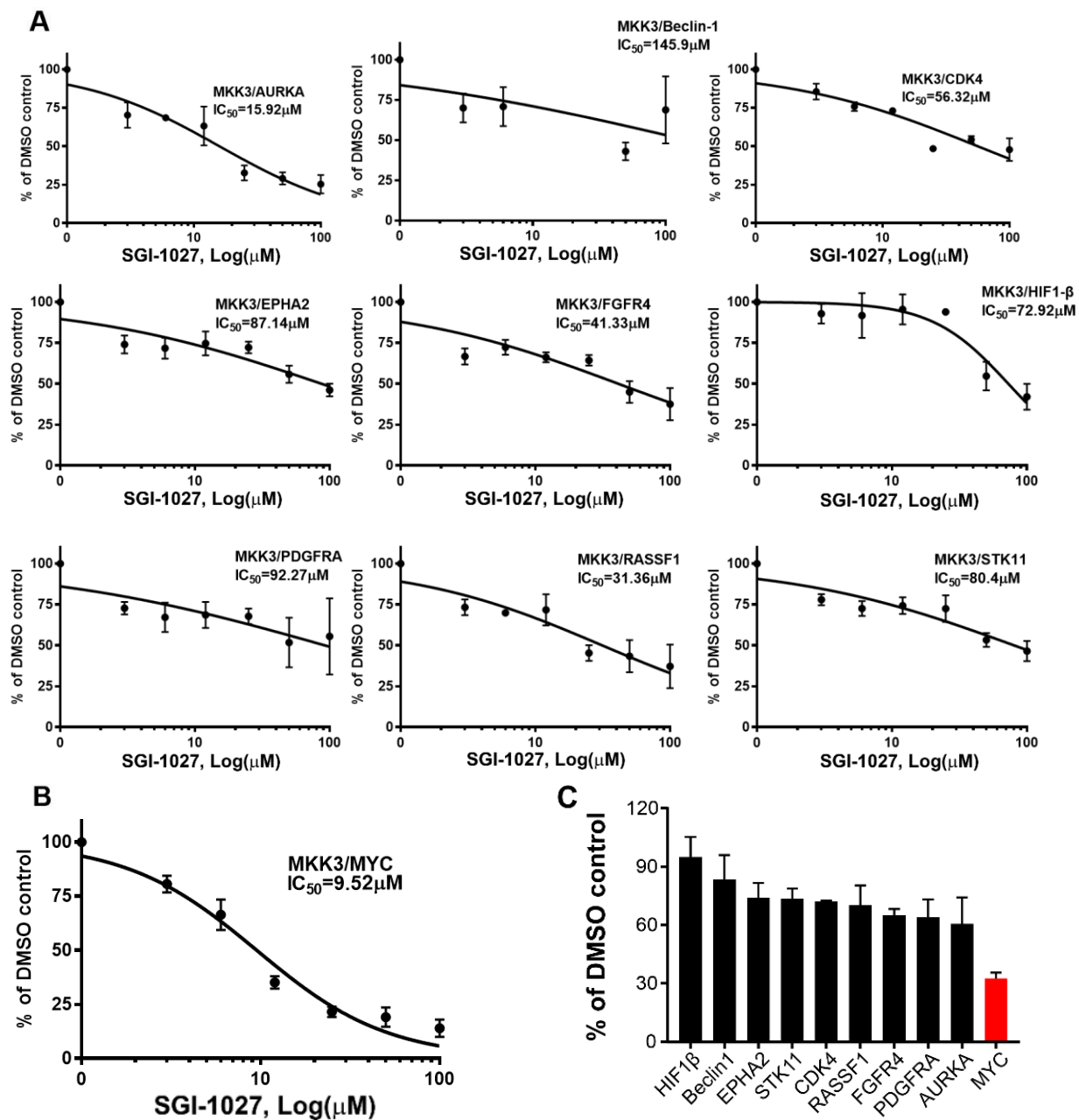


**Figure 17. SGI-1027 showed selectivity against other MKK3 PPIs.** A) The inhibitory effects of SGI-1027 on other nine pairs of MKK3 PPIs were tested in dose-response TR-FRET assay. All IC<sub>50</sub> values for those nine PPIs are higher than that for MKK3/MYC. B) Dose-response TR-FRET assay for MKK3/MYC PPI performed on the same day gave an IC<sub>50</sub>=9.52 μM, which is consistent with previous data. C) At a concentration of 12 μM, SGI-1027 treatment results in at least 70% inhibition on MKK3/MYC PPI. However, its effects on all other tested MKK3 PPIs were significantly less potent, ranging from 5% inhibition for MKK3/HIF1β to 40% inhibition for MKK3/AURKA.

other tested MKK3 PPIs was significantly less potent, and ranged from 5% inhibition for HIF1 $\beta$  to 40% inhibition for MKK3-AURKA PPI. Together, these results indicate that MKK3/MYC complex can be selectively targeted by small compounds without a disruption of other related PPIs.

### Computational modeling reveals SGI-1027-binding site on MKK3

Previous data suggest that MYC HLH binds to MKK3 cavity located in its small lobe around 121-135 residues<sup>31</sup>. To evaluate whether SGI-1027 also can favorably bind to this binding site on the MKK3 surface, our group applied a computational modeling approach. Based on the model obtained with the docking studies and refined by 100 ns molecular dynamics simulation the compound can favorably fit the MKK3 MYC-binding site (Fig. 18A). As shown in Fig. 18B, the quinoline moiety of SGI-1027 was located in a pocket formed by K105, M109, and L108, and the NH-group of the benzamide fragment forms a hydrogen bond with D112. The SGI-1027 amino pyrimidine moiety formed hydrogen bonds with the backbone atoms of Y127, T125, and V124. The computational modeling results support a direct interference of SGI-1027 with MKK3/MYC PPI interface and provide a structural basis for further experimental validation of SGI-1027 binding mode and rational design of new inhibitors for MKK3/MYC PPI.

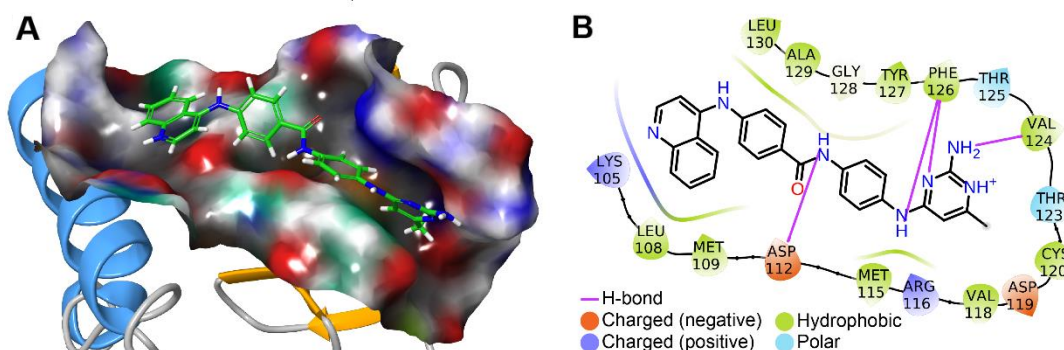


**Figure 18. Molecular computational modeling reveals SGI-1027-binding site on MKK3.** A) A model of SGI-1027 bound at MKK3 MYC-binding site. B) Molecular interactions between MKK3 and SGI-1027 identified based on the docking studies.

### **SGI-1027 suppresses MYC transcriptional activity and proliferation of cancer cell lines**

It has been shown that the binding of MKK3 to MYC leads to upregulation of MYC transcriptional activity<sup>31</sup>. Therefore, we tested whether this effect can be suppressed in the presence of SGI-1027. As shown in Fig 6A, in agreement with previous data<sup>31</sup>, overexpression of VF-MKK3 correlated with increased MYC transcriptional activity in a panel of cancer cell lines, including HCT116 and HT-29 colon cancer cells, MCF7 breast cancer cells, H1299 lung cancer cells, and MIA PaCa-2 pancreatic cancer cells as compared to Venus control. The MKK3-induced activation of MYC was suppressed by increasing concentration of SGI-1027 in a dose-dependent manner (Fig. 19A). Notably, SGI-1027 showed more dramatic effect on MYC activity in cells expressing VF-MKK3 comparing to the MYC activity detected from cells expressing Venus control. This observation further supports that SGI-1027 inhibits MYC activity through the disruption of MKK3/MYC PPI.

MYC is a master regulator of cell proliferation and inhibition of its transcriptional activity is expected to correlate with decreased cell proliferation<sup>23</sup>. Indeed, the results of the MYC reporter assay correlate with the dose-dependent inhibition of proliferation of HCT116, HT29, MCF7, MIA PaCa-2, and H1299 cells (Fig. 19B). We found that MYC activity and proliferation of HCT116 colon cancer cells were the most sensitive to SGI-1027, while lung cancer H1299 demonstrated a moderate sensitivity to SGI-1027 in both assays. Therefore, we tested the expression of MKK3 and MYC in the panel of cell lines tested. Blot for MKK3 and MYC in the cell lysates of the panel of cell lines showed that HCT116 cells have high expression of both MKK3 and MYC, while H1299 cells have relatively low level of MYC (Fig. 19C). The relative expression level of MKK3 and MYC in those cell lines has a strong correlation with their sensitivity to SGI-1027 in terms of MYC activity and cell proliferation.

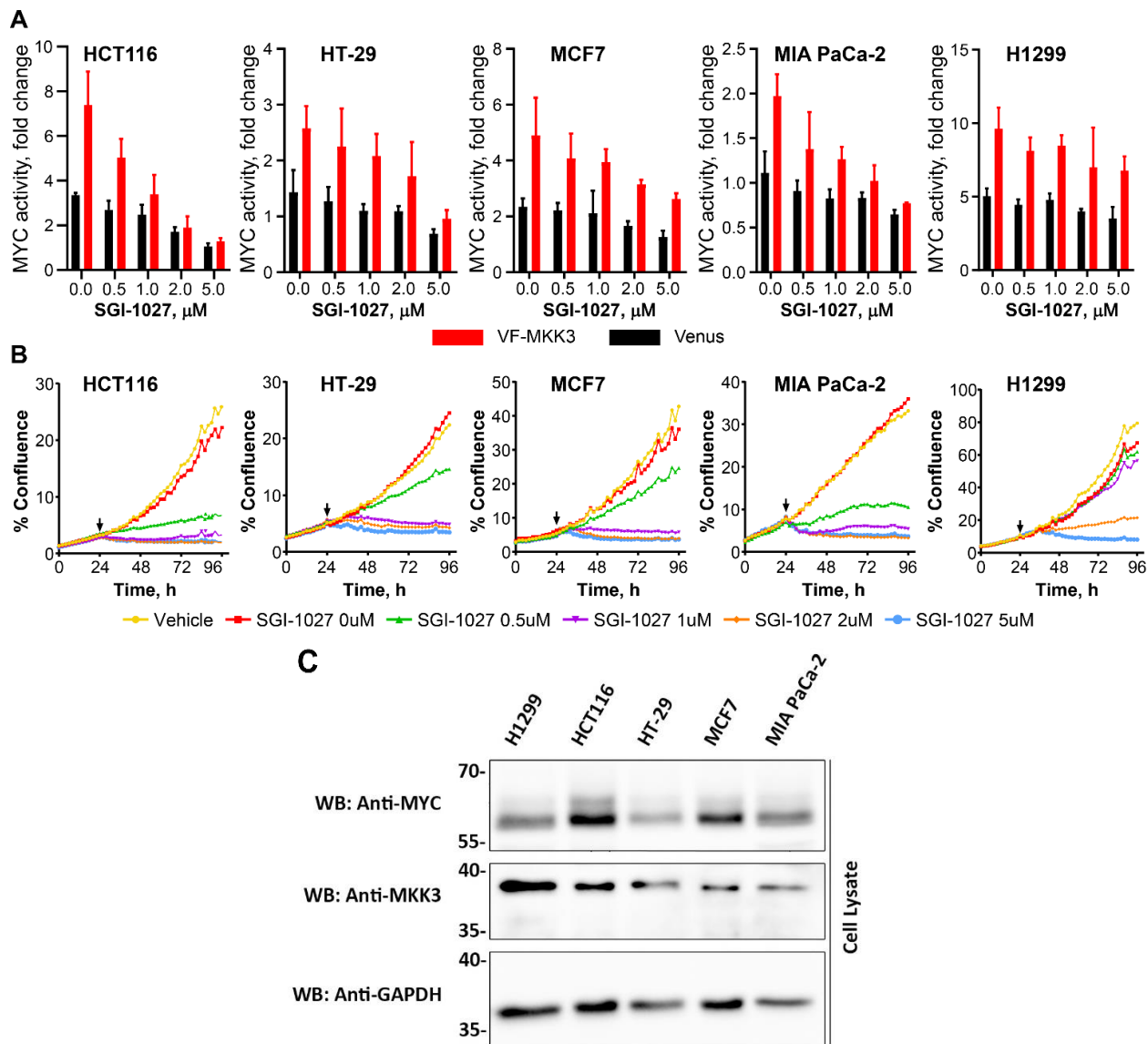


**Figure 19. SGI-1027 suppresses MYC transcriptional activity and proliferation of cancer cell lines.** A) MYC reporter assay was performed in a panel of cancer cell lines. Cells were transfected with VF-MKK3, EBOX reporter plasmid, and Renilla luciferase. Venus vector was used as negative control, and EBOX mutant served as negative control for the assay. 36 hours after transfection, cells were treated with SGI-1027 at assigned concentration and incubated for 12 hours. VF-MKK3 overexpression results in increased MYC activity, compared to Venus vector control. MKK3-induced MYC activation was suppressed by SGI-1027 in a dose-dependent manner. Meanwhile, SGI-1027 showed more dramatic effect on MYC activity in cells expressing VF-MKK3 comparing to the MYC activity detected from cells expressing Venus control. B) The effect of SGI-1027 on cell proliferation was tested in the panel of cancer cell lines using the IncuCyte live-cell analysis system. Cells were treated with SGI-1027 24 hours after being seeded into 384-well plates. Dose-dependent inhibition of proliferation was observed in all cell lines tested. The sensitivities of the cell lines to SGI-1027 treatment correlate with results from reporter assay. MYC activity and proliferation of HCT116 colon cancer cells were the most sensitive to SGI-1027, while lung cancer H1299 demonstrated a moderate sensitivity to SGI-1027 in both assays. C) Blot for endogenous expression level of MKK3 and MYC in the panel of cells tested showed that HCT116 cells have high expression of both MKK3 and MYC, which is in high agreement with the observation of HCT116 as most sensitive to SGI-1027 treatment in both MYC reporter assay and cell proliferation assay.

### **MKK3 knock-down results in decreased MYC transcriptional activity**

In order to further validate the on-target effect by SGI-1027, shRNA was used to generate MKK3 knock-down HCT116 cell lines. Two different shRNA, termed shRNA-75 and shRNA-85, packaged in lentiviral transduction particles were used. Western blot for whole cell lysates showed that MKK3 level was negligible in both knock-down cell lines, compared to HCT116 WT cells, indicating the high performance of the shRNA. Meanwhile, endogenous MYC level was also significantly lower in both knock-down cell lines (Fig. 20A), which is in excellent agreement with previous finding that MKK3 promotes MYC transcriptional activity. To further confirm the effect of MKK3 knock-down on MYC activity, MYC reporter assay was performed in both HCT116 WT and MKK3-KD cells. The result demonstrated that, compared to HCT116 WT cells, MKK3-KD cells have significantly lower MYC transcriptional activity (Fig. 20B). When VF-MKK3 was rescued back into MKK3-KD cells, significant increase of MYC activity was observed, compared to Venus vector control (Fig. 20C).

Together, these data suggest a strong correlation between MKK3 and MYC transcriptional activity, and also, HCT116 MKK3-KD cell lines provide an excellent platform for further validation of on-target effect by SGI-1027 on MKK3/MYC PPI.

### **Suppressive effect of SGI-1027 on MYC activity and cell proliferation correlates with inhibition of MKK3/MYC PPI**

Knowing that MYC activity is lower in HCT116 MKK3-KD cells, and this decrease can be rescued by MKK3 overexpression, the effect of SGI-1027 on MYC activity in MKK3-KD cells rescued with VF-MKK3 was tested in MYC reporter assay. The results first confirmed that VF-MKK3 overexpression can induce MYC activation in MKK3-KD cells. Meanwhile, this rescued MYC activation was suppressed by SGI-1027 at a low concentration of 2 $\mu$ M (Fig. 21A).

Effect of SGI-1027 on HCT116 WT and MKK3-KD cell proliferation was further tested using IncuCyte live-cell analysis system. Consistently, SGI-1027 showed significant and dose-dependent suppressive effect on HCT116 WT cell proliferation (Fig. 21B), but MKK3-KD cells were much less sensitive to SGI-1027 treatment (Fig. 21C).

Together, these data suggest that SGI-1027 suppresses MYC transcriptional activity and lead to decreased cell proliferation through inhibition of MKK3/MYC PPI.

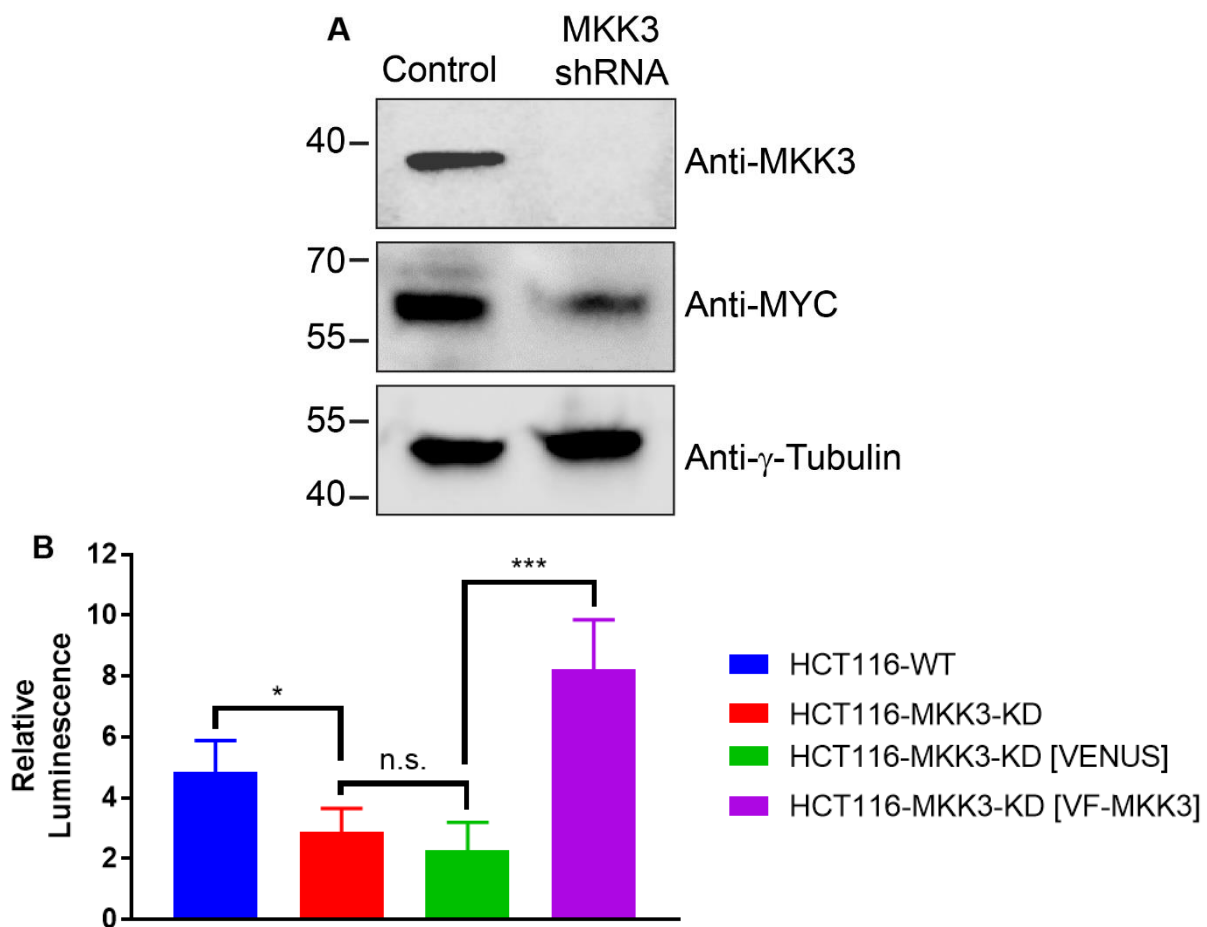


**Figure 20. MKK3 knock-down results in decreased MYC transcriptional activity.** A) HCT116 MKK3-KD cell line was generated using shRNA. Blot for whole cell lysate showed excellent performance of the shRNA. Endogenous MYC level was also significantly lower in MKK3-KD cells. B) Cells were transfected with VF-MKK3, EBOX reporter plasmid, and Renilla luciferase. Venus vector was used as negative control, and EBOX mutant served as negative control for the assay. MYC reporter assay showed that MYC activity is significantly lower in MKK3-KD cells, and this decrease can be rescued by MKK3 overexpression.

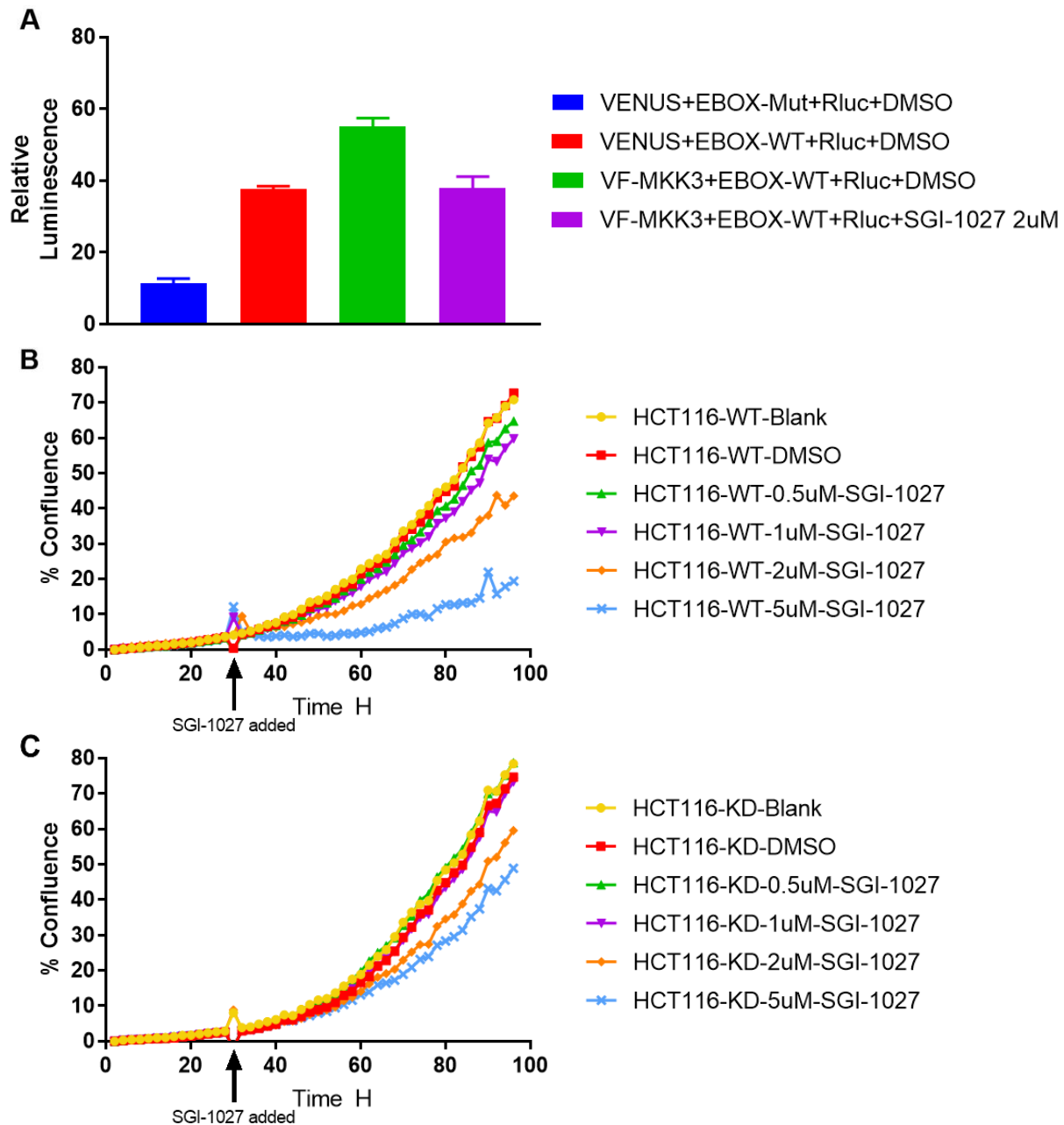


**Figure 21. Sensitivity of HCT116 cells to SGI-1027 is MKK3 dependent.** A) MYC reporter assay was performed on HCT116 MKK3-KD cells to evaluate the on-target effect of SGI-1027 on MKK3/MYC PPI. Overexpression of VF-MKK3 results in rescued MYC activity in MKK3-KD cells, and this rescued MYC activity was suppressed back with SGI-1027 treatment at 2 $\mu$ M for 12 hours. Venus and DMSO were used as negative controls, and EBOX mutant served as negative control for the assay. B) HCT116 WT cell proliferation under treatment of increasing concentration of SGI-1027 was monitored using the IncuCyte live-cell analysis system. After addition of SGI-1027, cell proliferation was significantly suppressed in a dose-dependent manner. C) After knocking down MKK3 in HCT116 cells, the cells become less sensitive to SGI-1027 treatment, indicating a strong correlation between the suppressive effect of SGI-1027 on cell proliferation and MKK3 expression.

## **Identification of potential regulators for MKK3/MYC PPI**

Though MKK3/MYC PPI has been validated as a promising target for therapeutic developments, mechanisms behind this crosstalk between MAP Kinase signaling pathway and MYC transcriptional program remains unclear. MKK3 is well known as the upstream activator of p38 MAPK, which plays a critical role in inflammation and apoptosis. However, we have shown that MKK3 can bind to MYC and leads to activation of MYC transcriptional program. How does MKK3 determine which direction to go?

To answer this question, we picked a panel of genes for regulators or binding partners of MKK3 and MYC. Venus-Flag fusions of these genes were co-expressed with GST-MKK3, and semi-endogenous pull-down assay was performed to evaluate their effect to MKK3/MYC PPI. Besides known binding between MKK3 and p38 as well as ASK1, interactions between MKK3 and ERK, GSK3 $\beta$ , HDAC1, STK38 were also observed (Fig. 22). Interestingly, when VF-GSK3 $\beta$  or VF-ASK1 was overexpressed, the interaction between GST-MKK3 and endogenous MYC was significantly inhibited.

## **ASK1 is a potential modulator of MKK3/MYC PPI**

ASK1 is the upstream activator of MKK3, and has been shown to have inhibitory effect on MKK3/MYC PPI. Therefore, the binding between MKK3 kinase-dead mutants and MYC was tested to see if MKK3 kinase activity is required for its interaction with MYC. The result indicates that both MKK3 kinase-dead mutants are still able to bind to MYC, indicating that MKK3/MYC PPI is independent of MKK3 kinase activity (Fig. 23A).

Knowing that ASK1 can be activated under oxidative stress, we used H<sub>2</sub>O<sub>2</sub> to treat MCF7 breast cancer cells to manipulate activation of endogenous ASK1. The result verified that ASK1

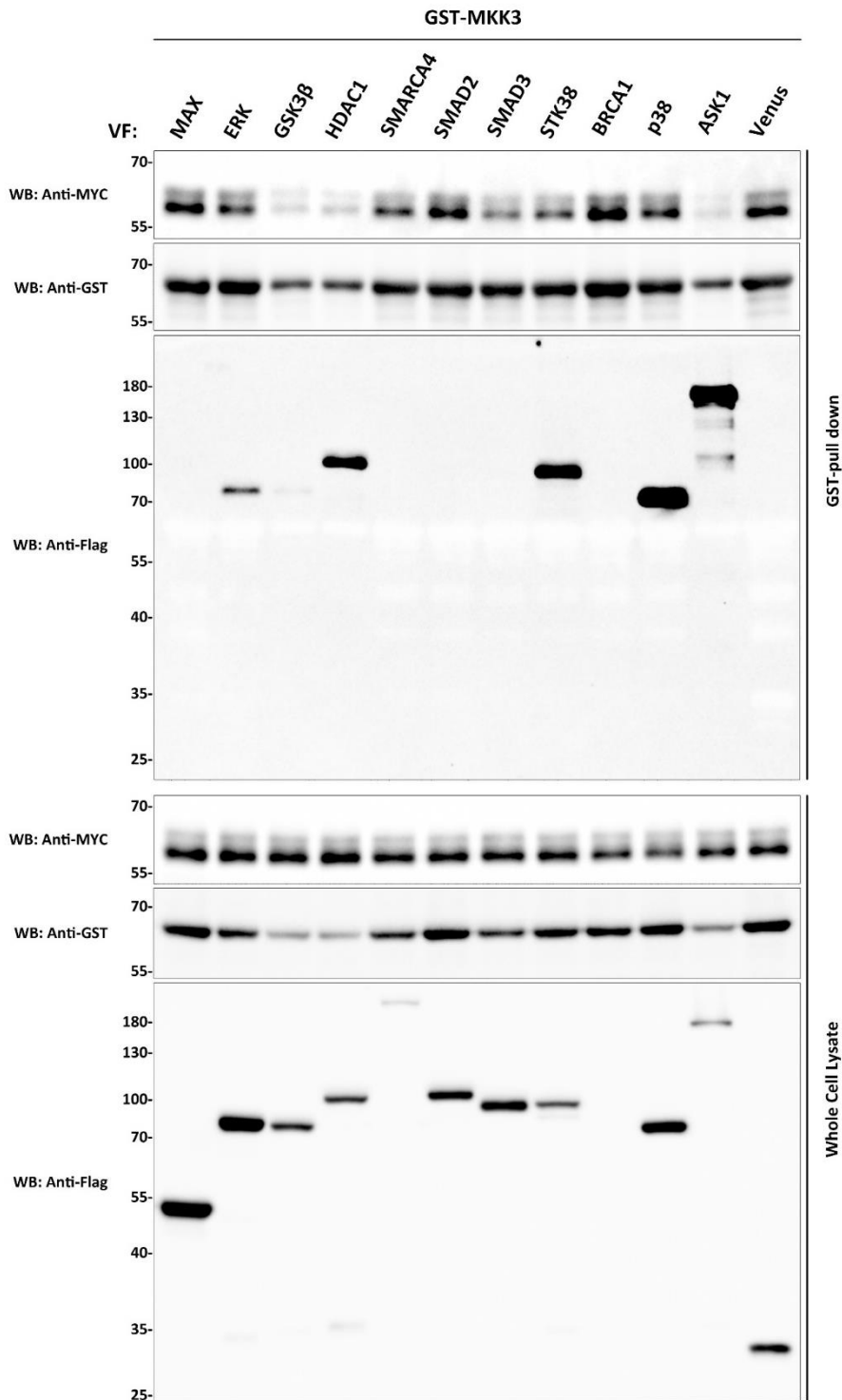


**Figure 22. ASK1 and GSK3 $\beta$  can inhibit MKK3/MYC PPI.** A panel of genes for known regulators or binding partners of MKK3 and MYC were co-expressed with GST-MKK3 in HEK293T cells. Semi-endogenous pull-down assay was performed to reveal their effects on interaction between GST-MKK3 and endogenous MYC. Venus vector served as a negative control. Besides identifying ERK, HDAC1, GSK3 $\beta$  and STK38 as new binding partners of MKK3, significant decrease of binding between GST-MKK3 and endogenous MYC was observed when ASK1, or GSK3 $\beta$ , or HDAC1 was co-expressed, indicating their inhibitory effect to MKK3/MYC PPI.

activation correlates with inhibition of MKK3/MYC PPI (Fig. 23B). When ASK1 is activated, it activates MKK3 through phosphorylation, which further activates p38 through phosphorylation. Meanwhile, ASK1 significantly inhibits MKK3/MYC PPI. Without MKK3-dependent MYC activation, endogenous MYC also significantly decreases.

Together, these data inspired a novel working model: When ASK1 is present and activated in cells, p38 pro-apoptotic direction is favored, and MKK3/MYC PPI is inhibited. When ASK1 is not activated or absent in cells, MKK3 would prefer to bind to MYC, resulting in activation of MYC transcriptional program (Fig. 23C).

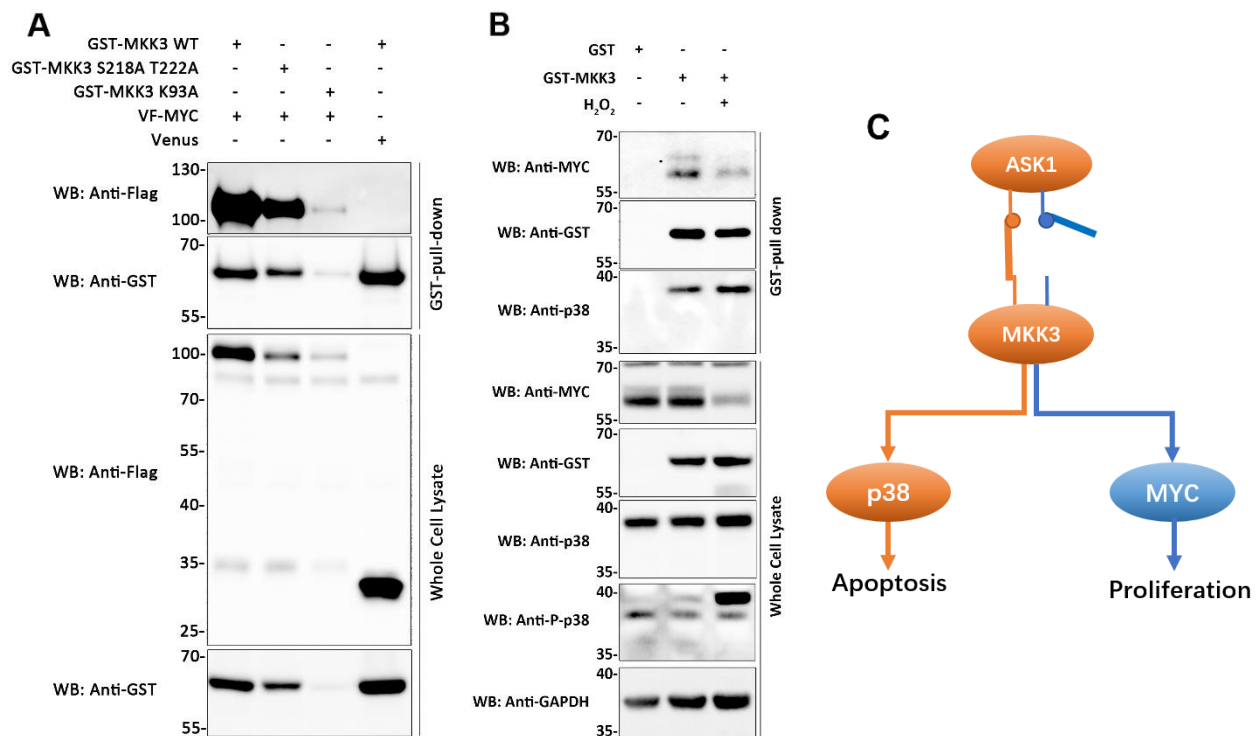


**Figure 23. ASK1 is verified as a potential modulator of MKK3/MYC PPI.** A) MKK3 kinase activity is not required for its interaction with MYC. VF-MYC was co-expressed with GST-MKK3 S218A T222A or GST-MKK3 K93A kinase-dead mutant in HEK293T cells. GST pull-down assay showed that both mutants can bind with MYC, indicating that MKK3/MYC PPI is independent of MKK3 kinase activity. GST-MKK3 WT was used as a positive control, and Venus vector served as a negative control for the assay. B) ASK1 activation results in inhibition of MKK3/MYC PPI and decreased level of MYC. MCF7 breast cancer cells were overexpressed with GST-MKK3 for 2 days, and treated with 3mM of H<sub>2</sub>O<sub>2</sub> for 1 hour to manipulate the activation of endogenous ASK1. Semi-endogenous pull-down assay was performed to test the effect of ASK1 activation to MKK3/MYC PPI. GST vector served as a negative control for the assay. C) Working model: When ASK1 is present and activated in cells, p38 pro-inflammatory and pro-apoptotic direction is favored, and MKK3/MYC PPI is inhibited. When ASK1 is not activated or absent in cells, MKK3 would prefer to bind to MYC, resulting in activation of MYC transcriptional program.

### **MKK3 interferes with MYC/GSK3 $\beta$ interaction**

GSK3 $\beta$  is widely known as a negative regulator of MYC, which promotes MYC degradation through phosphorylation. Interestingly, when VF-GSK3 $\beta$  was co-expressed with GST-MKK3 in cells, a significant decrease of endogenous MYC that bound to GST-MKK3 was observed (Fig. 22). Also, interaction between MKK3 and GSK3 $\beta$  was also observed. The binding between MKK3 and GSK3 $\beta$  was validated in a semi-endogenous pull-down assay, which demonstrates the interaction between GST-MKK3 and endogenous GSK3 $\beta$  (Fig. 24A). Meanwhile, no interaction between MKK3 and MAX could be detected, indicating that not all proteins can bind to GST-MKK3 in this assay, and thus the validity of this data.

To test the effect of MKK3 on MYC/GSK3 $\beta$  interaction, GST-GSK3 $\beta$  and VF-MKK3 were overexpressed in cells. Semi-endogenous pull-down assay revealed that with the presence of MKK3, the interaction between GSK3 $\beta$  and MYC is significantly decreased (Fig. 24B). Together with previous data that MKK3 binds to MYC and promotes MYC protein stability, another potential working model was developed: MKK3 inhibits the interaction between GSK3 $\beta$  and MYC, so that MYC degradation is blocked, and thus leads to higher stability of MYC protein (Fig. 24C).

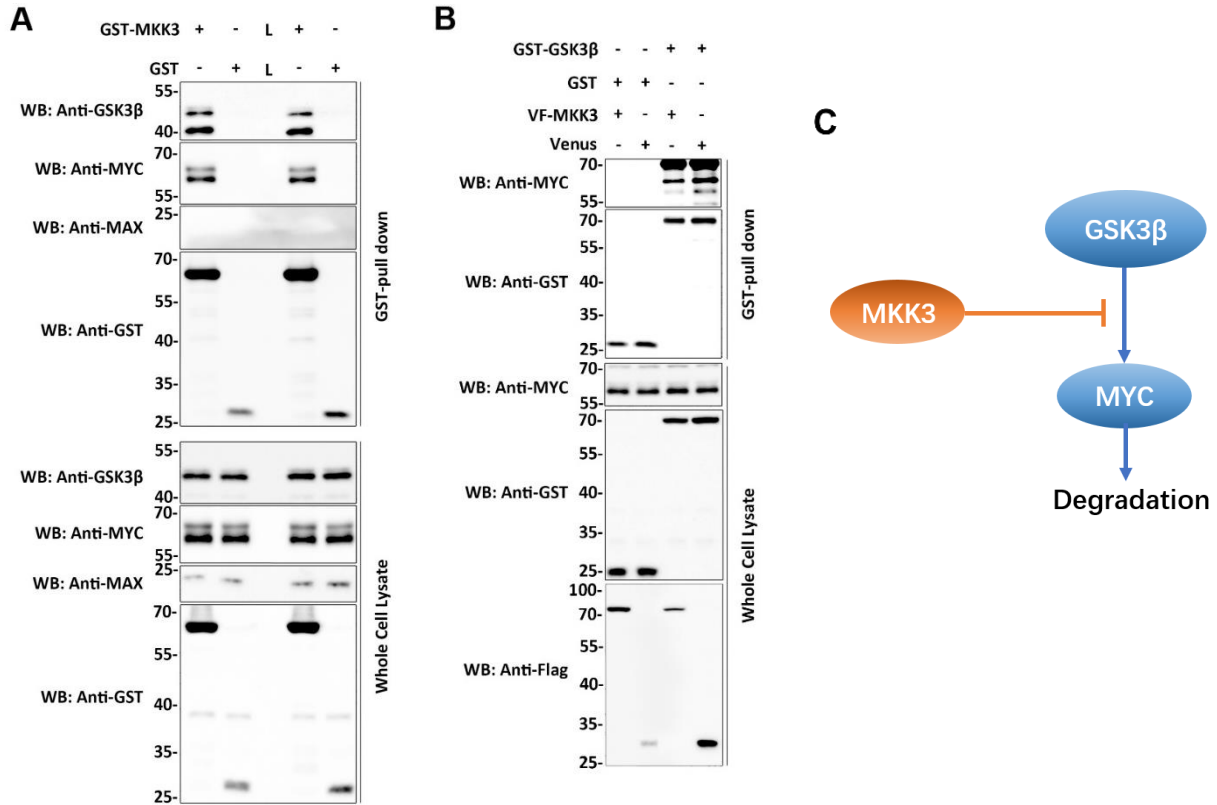


**Figure 24. MKK3 promotes MYC stability through inhibiting GSK3 $\beta$ -dependent MYC degradation.** A) Interaction between MKK3 and GSK3 $\beta$  was validated in a semi-endogenous pull-down assay. HEK293T cells were overexpressed with GST-MKK3, and the endogenous GSK3 $\beta$  precipitated with GST-MKK3 was detected through Western Blot. Meanwhile, no binding between MKK3 and MAX could be detected, indicating that not all proteins can bind to MKK3 in this assay, and thus the validity of this data. Two independent replicates are shown here. GST vector served as a negative control for the assay. L stands for protein ladder. B) MKK3 inhibits MYC/GSK3 $\beta$  interaction in a semi-endogenous pull-down assay. HEK293T cells were overexpressed with GST-GSK3 $\beta$  and VF-MKK3, and endogenous MYC precipitated with GST-GSK3 $\beta$  was detected through Western Blot. Venus vector was used as a positive control, and GST vector served as a negative control for the assay. C) Working model: MKK3 promotes MYC stability through inhibiting GSK3 $\beta$ -dependent MYC degradation.

## **Discussion**

Recently, through a PPI high-throughput screening combined with bioinformatics analysis of cancer genomics data our group has discovered the mitogen-activated protein kinase kinase 3 (MKK3 or MAP2K3) as a novel hub in the cancer-associated PPI network, termed OncoPPI<sup>30-32</sup>. MKK3 is a dual specificity threonine/tyrosine kinase known for its essential role in regulation of p38-activated inflammatory response to the stress signals<sup>35-37</sup>. On the other hand, there is growing evidence for multiple functions of MKK3 in regulation of cell viability beyond p38 inflammatory signaling<sup>38</sup>. For example, depletion of MKK3 was correlated with reduced cell proliferation and viability in breast cancer MCF7 cells and colon cancer HT29 and HCT116 cells<sup>38</sup>. The MKK3 gene knockdown resulted in significant inhibition of tumor growth in xenograft models<sup>39</sup>. Recently, Gossypetin is identified as a novel MKK3 and MKK6 inhibitor, and it has been shown that Gossypetin suppresses esophageal cancer growth *in vitro* and *in vivo*<sup>40</sup>. Thus, in addition to the regulation of p38-mediated inflammatory pathways, MKK3 exhibits pro-survival functions in different cancer models<sup>31,41</sup>. However, molecular mechanisms of MKK3-regulated cell growth and survival remain unclear. Our group showed that besides p38, MKK3 has a new role as binding partner and activator of the oncogenic master regulator MYC<sup>30-32</sup>.

To interrogate the functions of MKK3/MYC PPI, effective chemical probes are needed. First, based on previous discovery that MYC Helix-Loop-Helix domain (353-439) is responsible for its interaction with MKK3, shorter MYC truncations were designed and generated from the HLH domain as tools to further investigate the binding motif. We have shown that MYC 370-413 is sufficient for MKK3 binding, and can inhibit MKK3/MYC PPI in affinity pull-down assays. Overexpression of this 44-amino-acid peptide antagonist correlates with significant inhibition of cell proliferation and induction of cell death. Further generation and test of shorter MYC fragments narrowed the MKK3-binding domain on MYC down to 380-406, which has only 26 amino acids.

These data not only provide new insight into the mechanism and function of MKK3/MYC binding, but also demonstrate the feasibility to target MKK3/MYC PPI with chemical tools.

Then, to discover small molecule MKK3/MYC PPI inhibitors, a novel cell lysate-based TR-FRET assay in ultra-HTS 1536-well plate format was developed. The screening of ~6,000 diverse compounds from three compound libraries revealed several hits. The quinoline derivative SGI-1027 appeared as most potent disruptor of MKK3/MYC PPI inhibitor ( $IC_{50} = 8\mu M$ ), and its inhibitory activity was validated in multiple orthogonal assays. The computational modeling studies also suggest that SGI-1027 can bind to MKK3 binding site previously identified as its main binding site for MYC. Furthermore, SGI-1027 demonstrated a notable selectivity against other MKK3 and MYC PPIs, including their major MKK3-p38 and MYC-MAX PPIs.

The SGI-1027 attracts a growing attention as an effective inducer of apoptosis in different cancer cells<sup>42-44</sup>. Through biochemical studies SGI-1027 was defined as an inhibitor of DNMT1, DNMT3A, and DNMT3B DNA methyltransferases with the  $IC_{50}$  of 6 to 13  $\mu M$ <sup>44</sup> and thus, its tumor suppressive effects were also linked with the inhibition of DNMTs<sup>42-44</sup>. Our data revealed that besides DNMTs, SGI-1027 disrupts the MKK3/MYC complex in cells and *in vitro*.

Previously our group showed that MKK3 upregulates MYC transcriptional activity in HCT116 colon cancer cells and MCF7 breast cancer cells. In this study we have further validated the MKK3-induced MYC activation in HCT116, MCF7, and demonstrated the MKK3-induced MYC activity in colon cancer HT-29, lung cancer H1299, and pancreatic cancer MIA PaCa-2 cell lines. The upregulation of MYC by MKK3 was inhibited by SGI-1027 in a dose-dependent manner. Furthermore, the disruption of MKK3/MYC PPI and suppression of MYC activity by SGI-1027 correlates with the reduced proliferation of HCT116, HT29, MCF7, MIA PaCa2, and H1299 cell lines. Test for expression level of MKK3 and MYC in those cell lines suggests that HCT116 cells,

which are the most sensitive to SGI-1027 treatment in both MYC reporter assay and cell proliferation assay, have relatively high expression of both MKK3 and MYC. Together, these data indicate that the anti-tumor effects by SGI-1027 have a strong correlation with MKK3/MYC PPI inhibition.

SGI-1027 was previously discovered as an inhibitor of DNMTs, and this study adds MKK3/MYC PPI inhibition to its functions. To date, there is no evidence that DNMTs can upregulate MYC activity. Previous studies have also demonstrated that DNMT knock-down leads to decreased expression of MYC, indicating a negative regulatory effect of DNMTs on MYC<sup>45,46</sup>. Therefore, literature records support our finding of SGI-1027 as a promising MKK3/MYC PPI inhibitor by showing that DNMT inhibition does not harm MYC activity.

In conclusion, our studies have revealed the first-in-class small molecule MKK3/MYC PPI inhibitor to interrogate and control MYC-driven oncogenic programs in cancer cells. We showed that MKK3/MYC PPI interface is druggable and can be specifically disrupted by small molecule chemical tools. This study provides a new approach to regulated MYC activity through the inhibition of MKK3/MYC PPI and establishes a novel platform for the chemical probe discovery to interrogate MYC and MKK3 oncogenic PPI network.

On the other hand, even though it has been shown that MKK3 binds to MYC, promotes MYC transcriptional activity, and enhances MYC protein stability, the mechanism behind this crosstalk between MAP Kinase signaling pathway and MYC transcriptional program remains unclear. MKK3 is widely known as an upstream activator of p38 MAPK, whose activation results in activation of inflammation and apoptosis pathways. Meanwhile, our findings add MYC activation to the functions of MKK3, which is very distinct from its roles in MAPK pathways. Therefore, we aimed to answer two questions. First, how does MKK3 decide with direction to go,

p38 activation or MYC activation? Second, how does MKK3 promotes MYC transcriptional program?

We found that when the MKK3 activator, ASK1 (MAP3K5), is activated, the interaction between MKK3 and MYC is significantly diminished. Also, the independency of MKK3/MYC PPI and MKK3 kinase activity has been demonstrated. These findings inspired a novel working model: Working model: When ASK1 is present and activated in cells, p38 pro-inflammatory and pro-apoptotic direction is favored, and MKK3/MYC PPI is inhibited. When ASK1 is not activated or absent in cells, MKK3 would prefer to bind to MYC, resulting in evocation of MYC transcriptional program.

Furthermore, the negative regulator of MYC, GSK3 $\beta$ , was shown to have inhibitory effect on MKK3/MYC PPI. Interrogation of the relationship between MKK3 and GSK3 $\beta$ -induced MYC degradation revealed new function of MKK3 as an inhibitor to MYC/GSK3 $\beta$  interaction. Besides this, GSK3 $\beta$  has also been verified as a novel binding partner of MKK3. These findings suggest another working model: MKK3 promotes MYC stability through inhibiting GSK3 $\beta$ -dependent MYC degradation.

In conclusion, MKK3 promotes MYC transcriptional program through inhibiting the interaction between MYC and GSK3 $\beta$ , resulting in suppression of MYC degradation. However, when ASK1 is present and activated in the cells, MKK3 will be phosphorylated and, therefore, activated, leading to activation of p38 MAPK regulated pro-inflammatory and pro-apoptotic signaling pathways. When ASK1 is deleted or mutated, MKK3 cannot be activated, and cannot activate p38. Instead, MKK3 would prefer to bind with MYC, promote MYC transcriptional activity, enhance MYC protein stability, and result in MYC driven cell proliferation.

## Future Directions

Future investigation of MKK3/MYC PPI can be divided into three directions:

First, based on currently knowledge of MKK3 121-135 and MYC 380-406 as the domains responsible for MKK3/MYC PPI, mutagenesis can be performed in order to identify specific residues responsible for this interaction. Shorter version of inhibitory peptides can also be generated and used as tools to interrogate the PPI.

Second, since SGI-1027 has been validated as the first-in-class small molecule inhibitor against MKK3/MYC PPI, Structure-Activity Relationship (SAR) studies could be performed to develop SGI-1027 analogs with the hope to improve its potency, selectivity, water solubility, and so on. Even though there is no evidence that DNMTs can enhance MYC activity, it is crucial to remove the molecule's activity against DNMT while keeping its activity against MKK3/MYC PPI, in order to avoid potential off-target effects. Current data from molecular computational modeling studies might also provide basis for Structure based drug design (SBDD), which could potentially facilitate improvements of the MKK3/MYC PPI inhibitor. After the identification of better molecules, *in vivo* studies could be carried out in animal models. Then, ideally, the MKK3/MYC PPI inhibitor could be moved into clinical trials.

Last but not least, current progress on investigation about mechanisms behind the crosstalk between MAP Kinase signaling pathway and MYC transcriptional program still remains on the preliminary level. While small molecule inhibitor for this interaction has been identified, it is still important to understand the underlying molecular mechanisms of this PPI. It is important to keep in mind that small molecules not only help with therapeutic developments, but also, together with the peptide antagonist, provide tools for future chemical biology interrogation of MKK3/MYC PPI.

## **REFERENCES**

- 1 Ivanov, A. A., Khuri, F. R. & Fu, H. Targeting protein-protein interactions as an anticancer strategy. *Trends Pharmacol Sci* **34**, 393-400, doi:10.1016/j.tips.2013.04.007 (2013).
- 2 Schieven, G. L. The biology of p38 kinase: a central role in inflammation. *Current topics in medicinal chemistry* **5**, 921-928 (2005).
- 3 Nero, T. L., Morton, C. J., Holien, J. K., Wielens, J. & Parker, M. W. Oncogenic protein interfaces: small molecules, big challenges. *Nature reviews. Cancer* **14**, 248-262, doi:10.1038/nrc3690 (2014).
- 4 Scott, D. E., Bayly, A. R., Abell, C. & Skidmore, J. Small molecules, big targets: drug discovery faces the protein-protein interaction challenge. *Nat Rev Drug Discov* **15**, 533-550, doi:10.1038/nrd.2016.29 (2016).
- 5 Dang, C. V., Reddy, E. P., Shokat, K. M. & Soucek, L. Drugging the 'undruggable' cancer targets. *Nature reviews. Cancer* **17**, 502-508 (2017).
- 6 Modell, A. E., Blosser, S. L. & Arora, P. S. Systematic Targeting of Protein-Protein Interactions. *Trends Pharmacol Sci* **37**, 702-713 (2016).
- 7 Jin, L., Wang, W. & Fang, G. Targeting protein-protein interaction by small molecules. *Annu Rev Pharmacol Toxicol* **54**, 435-456, doi:10.1146/annurev-pharmtox-011613-140028 (2014).
- 8 Bretones, G., Delgado, M. D. & Leon, J. Myc and cell cycle control. *Biochim Biophys Acta* **1849**, 506-516, doi:10.1016/j.bbagr.2014.03.013 (2015).
- 9 Pereira, C. B. *et al.* MYC Amplification as a Predictive Factor of Complete Pathologic Response to Docetaxel-based Neoadjuvant Chemotherapy for Breast Cancer. *Clinical breast cancer* **17**, 188-194, doi:10.1016/j.clbc.2016.12.005 (2016).
- 10 Mollaoglu, G. *et al.* MYC Drives Progression of Small Cell Lung Cancer to a Variant Neuroendocrine Subtype with Vulnerability to Aurora Kinase Inhibition. *Cancer Cell* **31**, 270-285, doi:10.1016/j.ccell.2016.12.005 (2017).
- 11 Huang, W. *et al.* C-MYC overexpression predicts aggressive transformation and a poor outcome in mucosa-associated lymphoid tissue lymphomas. *International journal of clinical and experimental pathology* **7**, 5634-5644 (2014).
- 12 Wolfer, A. *et al.* MYC regulation of a "poor-prognosis" metastatic cancer cell state. *Proceedings of the National Academy of Sciences of the United States of America* **107**, 3698-3703, doi:10.1073/pnas.0914203107 (2010).
- 13 Ruzinova, M. B., Caron, T. & Rodig, S. J. Altered subcellular localization of c-Myc protein identifies aggressive B-cell lymphomas harboring a c-MYC translocation. *The American journal of surgical pathology* **34**, 882-891, doi:10.1097/PAS.0b013e3181db83af (2010).
- 14 Iwakawa, R. *et al.* MYC amplification as a prognostic marker of early-stage lung adenocarcinoma identified by whole genome copy number analysis. *Clinical cancer research : an official journal of the American Association for Cancer Research* **17**, 1481-1489, doi:10.1158/1078-0432.ccr-10-2484 (2011).
- 15 Alves Rde, C., Meurer, R. T. & Roehle, A. V. MYC amplification is associated with poor survival in small cell lung cancer: a chromogenic in situ hybridization study. *Journal of cancer research and clinical oncology* **140**, 2021-2025, doi:10.1007/s00432-014-1769-1 (2014).
- 16 Tansey, W. P. Mammalian MYC Proteins and Cancer. *New Journal of Science* **2014**, 27, doi:10.1155/2014/757534 (2014).
- 17 Wolfram, J. A., Lesnefsky, E. J., Hoit, B. D., Smith, M. A. & Lee, H. G. Therapeutic potential of c-Myc inhibition in the treatment of hypertrophic cardiomyopathy. *Therapeutic advances in chronic disease* **2**, 133-144, doi:10.1177/2040622310393059 (2011).
- 18 Hou, Y. *et al.* c-Myc is essential for urokinase plasminogen activator expression on hypoxia-induced vascular smooth muscle cells. *Cardiovascular research* **75**, 186-194, doi:10.1016/j.cardiores.2007.02.033 (2007).

- 19 de Nigris, F. *et al.* c-Myc oncoprotein: cell cycle-related events and new therapeutic challenges in cancer and cardiovascular diseases. *Cell cycle (Georgetown, Tex.)* **2**, 325-328 (2003).
- 20 Lee, H. G. *et al.* The neuronal expression of MYC causes a neurodegenerative phenotype in a novel transgenic mouse. *The American journal of pathology* **174**, 891-897, doi:10.2353/ajpath.2009.080583 (2009).
- 21 Lee, H. P., Kudo, W., Zhu, X., Smith, M. A. & Lee, H. G. Early induction of c-Myc is associated with neuronal cell death. *Neuroscience letters* **505**, 124-127, doi:10.1016/j.neulet.2011.10.004 (2011).
- 22 Raj, K. & Sarkar, S. Transactivation Domain of Human c-Myc Is Essential to Alleviate Poly(Q)-Mediated Neurotoxicity in Drosophila Disease Models. *Journal of molecular neuroscience : MN* **62**, 55-66, doi:10.1007/s12031-017-0910-4 (2017).
- 23 Adhikary, S. & Eilers, M. Transcriptional regulation and transformation by Myc proteins. *Nature reviews. Molecular cell biology* **6**, 635-645, doi:10.1038/nrm1703 (2005).
- 24 Tu, W. B. *et al.* Myc and its interactors take shape. *Biochimica et biophysica acta* **1849**, 469-483, doi:10.1016/j.bbagr.2014.06.002 (2015).
- 25 Yeh, E. *et al.* A signalling pathway controlling c-Myc degradation that impacts oncogenic transformation of human cells. *Nat Cell Biol* **6**, 308-318, doi:10.1038/ncb1110 (2004).
- 26 Nair, S. K. & Burley, S. K. X-ray structures of Myc-Max and Mad-Max recognizing DNA. Molecular bases of regulation by proto-oncogenic transcription factors. *Cell* **112**, 193-205 (2003).
- 27 Prochownik, E. V. & Vogt, P. K. Therapeutic Targeting of Myc. *Genes Cancer* **1**, 650-659, doi:10.1177/1947601910377494 (2010).
- 28 Jung, K. Y. *et al.* Perturbation of the c-Myc-Max protein-protein interaction via synthetic alpha-helix mimetics. *Journal of medicinal chemistry* **58**, 3002-3024, doi:10.1021/jm501440q (2015).
- 29 Fletcher, S. & Prochownik, E. V. Small-molecule inhibitors of the Myc oncoprotein. *Biochimica et biophysica acta* **1849**, 525-543, doi:10.1016/j.bbagr.2014.03.005 (2015).
- 30 Li, Z. *et al.* The OncoPPI network of cancer-focused protein-protein interactions to inform biological insights and therapeutic strategies. *Nat Commun* **8**, 14356, doi:10.1038/ncomms14356 (2017).
- 31 Ivanov, A. A. *et al.* OncoPPI-informed discovery of Mitogen-Activated Protein Kinase Kinase 3 as a novel binding partner of c-Myc. *Oncogene* **36**, 5852-5860, doi:doi:10.1038/onc.2017.180 (2017).
- 32 Ivanov, A. A. *et al.* The OncoPPI Portal: an integrative resource to explore and prioritize protein-protein interactions for cancer target discovery. *Bioinformatics (Oxford, England)* **34**, 1183-1191, doi:10.1093/bioinformatics/btx743 (2018).
- 33 Xiong, J. *et al.* Development of a Time-Resolved Fluorescence Resonance Energy Transfer Ultrahigh-Throughput Screening Assay for Targeting the NSD3 and MYC Interaction. *Assay Drug Dev Technol* **16**, 96-106, doi:10.1089/adt.2017.835 (2018).
- 34 Mo, X. *et al.* HTiP: High-Throughput Immunomodulator Phenotypic Screening Platform to Reveal IAP Antagonists as Anti-cancer Immune Enhancers. *Cell chemical biology*, doi:10.1016/j.chembiol.2018.11.011 (2018).
- 35 Kim, E. K. & Choi, E. J. Pathological roles of MAPK signaling pathways in human diseases. *Biochimica et biophysica acta* **1802**, 396-405, doi:10.1016/j.bbadis.2009.12.009 (2010).
- 36 Inoue, T. *et al.* Mitogen-activated protein kinase kinase 3 is a pivotal pathway regulating p38 activation in inflammatory arthritis. *Proceedings of the National Academy of Sciences of the United States of America* **103**, 5484-5489, doi:10.1073/pnas.0509188103 (2006).
- 37 Kasuya, Y., Umezawa, H. & Hatano, M. Stress-Activated Protein Kinases in Spinal Cord Injury: Focus on Roles of p38. *Int J Mol Sci* **19** (2018).

- 38 Gurtner, A. *et al.* Mutant p53-induced up-regulation of mitogen-activated protein kinase kinase 3 contributes to gain of function. *The Journal of biological chemistry* **285**, 14160-14169 (2010).
- 39 Baldari, S., Ubertini, V., Garufi, A., D'Orazi, G. & Bossi, G. Targeting MKK3 as a novel anticancer strategy: molecular mechanisms and therapeutical implications. *Cell death & disease* **6**, e1621, doi:10.1038/cddis.2014.591 (2015).
- 40 Xie, X. *et al.* Gossypetin is a novel MKK3 and MKK6 inhibitor that suppresses esophageal cancer growth in vitro and in vivo. *Cancer Lett* **442**, 126-136, doi:10.1016/j.canlet.2018.10.016 (2019).
- 41 Bossi, G. MKK3 as oncotarget. *Aging (Albany NY)* **8**, 1-2 (2016).
- 42 Sun, N., Zhang, J., Zhang, C., Zhao, B. & Jiao, A. DNMTs inhibitor SGI-1027 induces apoptosis in Huh7 human hepatocellular carcinoma cells. *Oncology letters* **16**, 5799-5806, doi:10.3892/ol.2018.9390 (2018).
- 43 Manara, M. C. *et al.* A Quinoline-Based DNA Methyltransferase Inhibitor as a Possible Adjuvant in Osteosarcoma Therapy. *Molecular cancer therapeutics* **17**, 1881-1892, doi:10.1158/1535-7163.mct-17-0818 (2018).
- 44 Datta, J. *et al.* A new class of quinoline-based DNA hypomethylating agents reactivates tumor suppressor genes by blocking DNA methyltransferase 1 activity and inducing its degradation. *Cancer research* **69**, 4277-4285, doi:10.1158/0008-5472.can-08-3669 (2009).
- 45 Brenner, C. *et al.* Myc represses transcription through recruitment of DNA methyltransferase corepressor. *EMBO J* **24**, 336-346, doi:10.1038/sj.emboj.7600509 (2005).
- 46 Poole, C. J. *et al.* DNMT3B overexpression contributes to aberrant DNA methylation and MYC-driven tumor maintenance in T-ALL and Burkitt's lymphoma. *Oncotarget* **8**, 76898-76920, doi:10.18632/oncotarget.20176 (2017).